2014

Legacy Phosphorus Implications in the Lake Pontchartrain Estuary Sediment Due to the 2011 Bonnet Carre Spillway Opening

Nhan Thanh Nguyen
Louisiana State University and Agricultural and Mechanical College

LEGACY PHOSPHORUS IMPLICATIONS IN THE LAKE PONTCHARTRAIN ESTUARY SEDIMENT DUE TO THE 2011 BONNET CARRÉ SPILLWAY OPENING

A Thesis

Submitted to the Graduate Faculty of the
Louisiana State University and
Agricultural and Mechanical College
in partial fulfillment of the
requirements for the degree of
Master of Science

in

The Department of Oceanography and Coastal Sciences

by
Nhan Thanh Nguyen
B.S., Louisiana State University, 2012
December 2014

ACKNOWLEDGEMENTS

This research and thesis benefited from efforts by many individuals that deserve recognition. I would like to sincerely acknowledge my major advisor, Dr. John R. White, for giving me the opportunity to pursue my interests in water quality research; and also his mentorship and guidance throughout my graduate and undergraduate studies. I would also like to thank my committee members; Dr. Eric Roy for his knowledge and expertise in this research, and Dr. Kehui Xu, for assisting me with grain size analysis in the Sediment Dynamics Lab and producing the spatial sediment characteristic plots. I would like to also thank my fellow graduate students for their assistance and support throughout the years. Finally, I wish to express my gratitude to my friends, families and most importantly my parents who have motivated me and stood by my side throughout this strenuous process.

TABLE OF CONTENTS

ACKNOWLEDGEMENTS…….....ii

LIST OF TABLES……...……v

LIST OF FIGURES……vi

LIST OF EQUATIONS…….....viii

ABSTRACT…….....…ix

CHAPTER ONE: REVIEW OF LITERATURE……1
1.1 2011 Mississippi River Flood Event Impact……..…….....1
1.2 Bonnet Carré Spillway…….....…..3
1.3 Phosphorus and Internal P Loading…….....….9
1.4 Phosphorus Fractionation…….....11

CHAPTER TWO: EFFECTS OF THE 2011 BONNET CARRÉ SPILLWAY OPENING ON SEDIMENT PROPERTIES AND PHOSPHORUS FORMS IN THE LAKE PONTCHARTRAIN ESTUARY……..13
2.1 Introduction…….…….....13
2.2 Phosphorus Forms: Organic and Inorganic P…….…….....15
2.3 Materials and Methods……..……...…….17
2.3.1 Site Study……...…….……...17
2.3.2 Sampling and Sediment Characteristics…….…….....18
2.3.3 Total Phosphorus- [TP] and Metal Analysis……..20
2.3.4 Phosphorus Fractionations…….....….....21
2.4 Results and Discussion……...…….……...25
2.4.1 Grain Size Analysis……...…….....27
2.4.2 Phosphorus Fractionations……...…….…….....31
2.5 Conclusion…….…….....35

CHAPTER THREE: POTENTIAL PHOSPHORUS LEGACY OF THE 2011 BONNET CARRÉ SPILLWAY OPENING ON LAKE PONTCHARTRAIN PHOSPHORUS CYCLING……..38
3.1 Introduction ...……...……....38
3.2 Accumulation of P in the Sediment....…….…...41
3.3 Methods …...……...…….…….44
3.4 Results ...……...……47
3.4.1 Relationship of P Concentrations in Comparison with Distance...47
3.4.2 Phosphorus Flux Estimation....…….……...……..48
3.5 Conclusion....…….55

CHAPTER FOUR: CONCLUSIONS……..57

LITERATURE CITED…...…….……58

APPENDIX A: MOISTURE CONTENT RELATIOSHIP VS. DISTANCE FROM THE BCS……...……....63

APPENDIX B: BULK DENSITY RELATIOSHIP VS. DISTANCE FROM THE BCS……....64

APPENDIX C: LOSS ON IGNITION RELATIOSHIP VS. DISTANCE FROM THE BCS……..……..65

APPENDIX D: TOTAL CARBON CONCENTRATION RELATIOSHIP VS. DISTANCE FROM THE BCS……..…66

APPENDIX E: TOTAL NITROGEN CONCENTRATION RELATIOSHIP VS. DISTANCE FROM THE BCS…….....67

APPENDIX F: TOTAL PHOSPHORUS CONCENTRATION RELATIOSHIP VS. DISTANCE FROM THE BCS…….....68

APPENDIX G: READILY AVAILABLE P CONCENTRATION RELATIOSHIP VS. DISTANCE FROM THE BCS……..69

APPENDIX H: ALKALI ORGANIC P CONCENTRATION RELATIOSHIP VS. DISTANCE FROM THE BCS……..70

APPENDIX I: FE/AL BOUND P CONCENTRATION RELATIOSHIP VS. DISTANCE FROM THE BCS……..71

APPENDIX J: CA/MG BOUND P CONCENTRATION RELATIOSHIP VS. DISTANCE FROM THE BCS……..72

APPENDIX K: RESIDUAL P CONCENTRATION RELATIOSHIP VS. DISTANCE FROM THE BCS……...……73

VITA.……...…….....74

LIST OF TABLES

Table 1.1. Operation of the Bonnet Carré Spillway since construction in 1932. All 10 BCS opening events are listed with the maximum flow capacity and the total water discharged……....5

Table 1.2. Three most recent Bonnet Carré Spillway openings with the amount of hydraulic and sediment loading. The total dissolved inorganic nutrients loading include dissolved inorganic nitrogen and dissolved inorganic phosphorus (Roy et al., 2013)…….……...8

Table 2.1. Sediment characteristics and mean ± 1 standard deviation from the 0-5 cm and 5-10 cm segment intervals before and after the 2011 Bonnet Carré Spillway opening. Student's T tests were used to test significance at $\alpha < 0.05$. The asterisks represent significance between pre-opening and post-close of the spillway..……...26

Table 2.2. Average P concentration (mg kg^{-1}) from 0-5 cm and 5-10 cm segment intervals and the percentage change before and after the 2011 BCS event, standard deviation, and the percent change of each P pool. (*significant level $P < 0.05$ from a Student's T test)…….……...32

Table 3.1. Various pools of Net P concentration from 0-10 cm segment intervals due to the 2011 Bonnet Carré Spillway event. The percent change of each pool before and after the BCS closure and the amount of time it takes for the new P to flux out from the sediment based on 517 Mt y^{-1} mean flux rate (Roy et al., 2012)……..……...51

LIST OF FIGURES

Figure 1.1: Map of the Mississippi River Basin water shed and tributaries inflow into the Mississippi River. (US Army Corp of Engineers, 2012)…..…….....2

Figure 1.2: Map of the southern Lake Pontchartrain estuary. The locations of the Mississippi River, the Bonnet Carré Spillway diversion, and the city of New Orleans are shown. Lake Borgne is connected to the LPE via the Chef Menteur Pass and the Rigolets……..…..…3

Figure 1.3. The Bonnet Carré Spillway structure with two cranes pulling the pin-like timbers to allow water flow from the Mississippi River into the Lake Pontchartrain Estuary (USACE, 2011)……...……..……...……4

Figure 1.4 a,b,c. MODIS Aqua Reflectance of the sediment rich floodwater inputted due to the opening of the BCS. A) 3 days before the BCS opening B) 8 days after the BCS opened C) 20 days after the BCS opened in 2011.…….…..…7

Figure 2.1. Map of the Lake Pontchartrain estuary. The locations of the Mississippi River, the Bonnet Carré Spillway diversion, and the city of New Orleans are shown. Lake Borgne is connected to the Lake Pontchartrain estuary via the Chef Menteur Pass and the Rigolets. (Source: Google Earth)…….17

Figure 2.2. Areal map of the Lake Pontchartrain estuary. The locations of Mississippi River and the Bonnet Carré Spillway are shown. The sampling locations are represented by the dots. Suspended sediment concentrations are represented in the red plume at 547nm reflectance (Naval Research Laboratory, Stennis Space Center, MS....19

Figure 2.3. Phosphorus sequential extraction scheme according to the bioavailability of P……...…….....22

Figure 2.4. Grain Size of sand, silt, and clay at each station from the 0-5 cm sediment interval for preopening (left) and post closure (right)……...… ……..28

Figure 2.5. Grain Size of sand, silt, and clay at each station from the 5-10 cm sediment interval for preopening (left) and post closure (right)…… …….……....29

Figure 2.6. Mean P concentration (mg kg^{-1}) of various P fractionations of 0-5 cm and 5-10 cm sediment intervals before and after the closure of the BCS and standard deviation of the total P pools. Student's t test $P < 0.05$ denotes significant level is shown with the star symbol……..……..…..……34

Figure 3.1. Diagram of various forms of P, pools and transformation pathways of P in the Lake Pontchartrain estuary (Rates are defined in the main text)….. ……..…....42

Figure 3.2: Before the 2011 BCS opening P fractions concentrations in correlation From the distance of the BCS mouth of Fe/Al bound P at A) 0-5cm and B) 5-10cm; Ca/Mg bound P at C) 0-5 cm and D) 5-10 cm; and Residual P at E) 0-5 cm and F) 5-10 cm sediment intervals……..……...……...49

Figure 3.3. 2011 BCS post closure P fractions concentrations in correlation from the distance of the BCS mouth of Fe/Al bound P at A) 0-5cm and B) 5-10cm; Ca/Mg bound P at C) 0-5 cm and D) 5-10 cm; and Residual P at E) 0-5 cm and F) 5-10 cm sediment interval……..……..……..…….....50

Figure 3.4. Time duration of potential internal phosphorus loading from Lake Pontchartrain sediments based on different assumptions (α) before the 2011 Bonnet Carré Spillway Event……....53

Figure 3.5. Linear flux rate estimate of the newly added TP from the 0-10 cm sediment interval after the closure of the 2011 Bonnet Carré Spillway……...55

LIST OF EQUATIONS

Equation 2.1: NaOH [TP] = NaOH [P_i] + NaOH [P_o]……..……..……24

Equation 3.1. $J = -D\ \frac{\partial \phi}{\partial x}$……...……..…..…45

Equation 3.2.

$$TPmass = (TP)\ x\ (Bulk\ Density)\ x\ (\ Volume\ of\ Lake\ Sediment)$$……..45

Equation 3.3.

$$\text{Years of DIP Flux} = \frac{(\text{TPmass } 0-10 \text{ cm})\ \text{x}\ (\%\ \text{Reactive P})(\alpha)}{(\text{Mean DIP flux rate})}$$…….……...…..46

ABSTRACT

Phosphorus (P) is an essential nutrient for life and excess P in aquatic systems can trigger algal blooms. Nutrient-rich Mississippi River water is diverted into the Lake Pontchartrain estuary (LPE) periodically through the Bonnet Carré Spillway (BCS) to avoid downstream flooding to the city of New Orleans, Louisiana and can significantly increase the internal P load in the sediment. A sequential P fractionation procedure was performed on sediments collected before the opening and after the closing of the 2011 BCS operation to understand the role of these large river diversions on P dynamics. Before the 2011 BCS opening, 10,368 Mt of P were found in the 0-10 cm sediment interval of the LPE. After the closure of the spillway, 13,293 Mt of P were measured in the 0-10 cm sediment interval. Total P significantly increased by 28% and a mass loading of 2,925 Mt of P was a consequence of the 42 days BCS opening. Sediment grain size analyzes revealed that majority of the finer sand and silt fractions were deposited near the BCS entrance, while the lighter clay fraction were transported tens of km towards the center of the LPE.

Calculating the time for all newly added P from the 2011 BCS operation to flux out of the water column is important to understanding the impact on water quality of the LPE. Using a previously determined linear flux rate of ~517 Mt yr^{-1}, it was estimated that ~6 years are needed to flux out the newly added sediment TP. While assuming a nonlinear model of flux rate, it is suggested that it would take a longer period of time to flux out all the newly P loaded from the sediments in the LPE. If the operations of these BCS opening are closely spaced in time (< 6 years), there will be an increase of P in the sediments which could lead to changes in the trophic status of the LPE. This increase of

TP in sediments can lead to an increase in the frequency and persistence of harmful algal blooms for many years after the spillway opening.

CHAPTER ONE: REVIEW OF LITERATURE

1.1 2011 Mississippi River Flood Event Impact

The Mississippi River flood in 2011 was one of the most substantial flooding disasters in U.S. history causing over 2 billion U.S. dollars in damages, since the Great Flood of 1927. Excessive seasonal snow melt and rainfall in the Mississippi River (MSR) watershed flow southward toward the Gulf of Mexico in spring and early summer of 2011. Record flooding was observed in cities along the Mississippi River main channel which threatened to flood over the Mississippi River banks and levee systems. The U.S. Army Corp of Engineers planned to divert floodwater away from large settlements through the blasting of levees and flooding of agricultural lands as well as the opening of diversions and spillways. For the first time in 37 years, the Morganza Spillway was opened to divert floodwater flow into a 12,000 km^2 rural area and towards the Atchafalaya Basin to relief flooding pressure in Baton Rouge, the capital of Louisiana. The Bonnet Carré Spillway (BCS) was opened on May 9, 2011 and closed on June 20, 2011 for a duration of 42 days to help alleviate floodwaters from threatening the city of New Orleans.

The Mississippi River Basin is the largest river drainage system in the United States. It covers nearly 40% of the continental U.S. and spreads to 31 states. The 3,766 km long MSR runs from Lake Itasca in Minnesota and empties out into the Gulf of Mexico (Fig. 1.1). The annual average water discharge rate is 16,792 m^3 per second. Depending on the time of the year; the rate can range from 4,502 $m^3 s^{-1}$ in fall to 86,791 $m^3 s^{-1}$ at its peak during spring flooding events. Seasonal flooding historically provided a

bulk of water, sediment and nutrients onto distributaries systems along the coast, estuaries, lake systems and to the Gulf of Mexico.

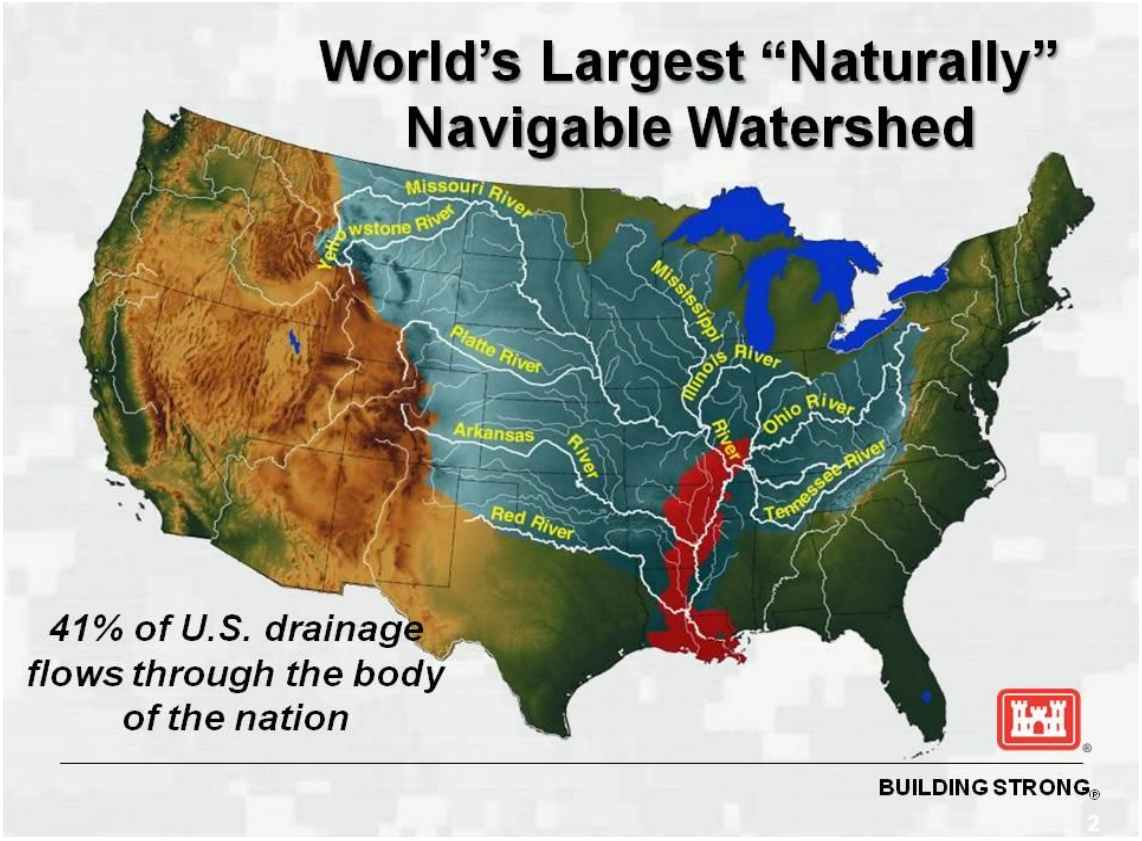

Figure 1.1. Map of the Mississippi River Basin watershed and distributaries inflow into the Mississippi River. (US Army Corp of Engineers, 2013)

Over the last century, nearly 1.3 million square miles of the Mississippi River watershed has experienced major changes, including conversion of more than 80 percent of forested wetlands to agriculture and urban areas and construction of dams and levees. These massive structures trap sediment and freshwater supply to the natural flood plain by preventing the river from switching courses or overtopping its banks. There are now ~ 8,000 dams and levees along the Mississippi River system (Blum and Roberts, 2009). Since the early 1950s, the U.S. government has worked on the Old River Control

Structure to prevent the MSR from switching to the Atchafalaya River basin. The decision was made to control the river so that 70 % of the year-round discharge would flow to the MSR and the remaining 30 % would flow into the Atchafalaya River (Allison et al., 2011).

1.2 Bonnet Carré Spillway

In response to the Great Flood of 1927, the Mississippi River Commission designed and constructed the BCS as part of the Mississippi River and Tributaries Project to prevent flooding to the Lower Mississippi River Basin.

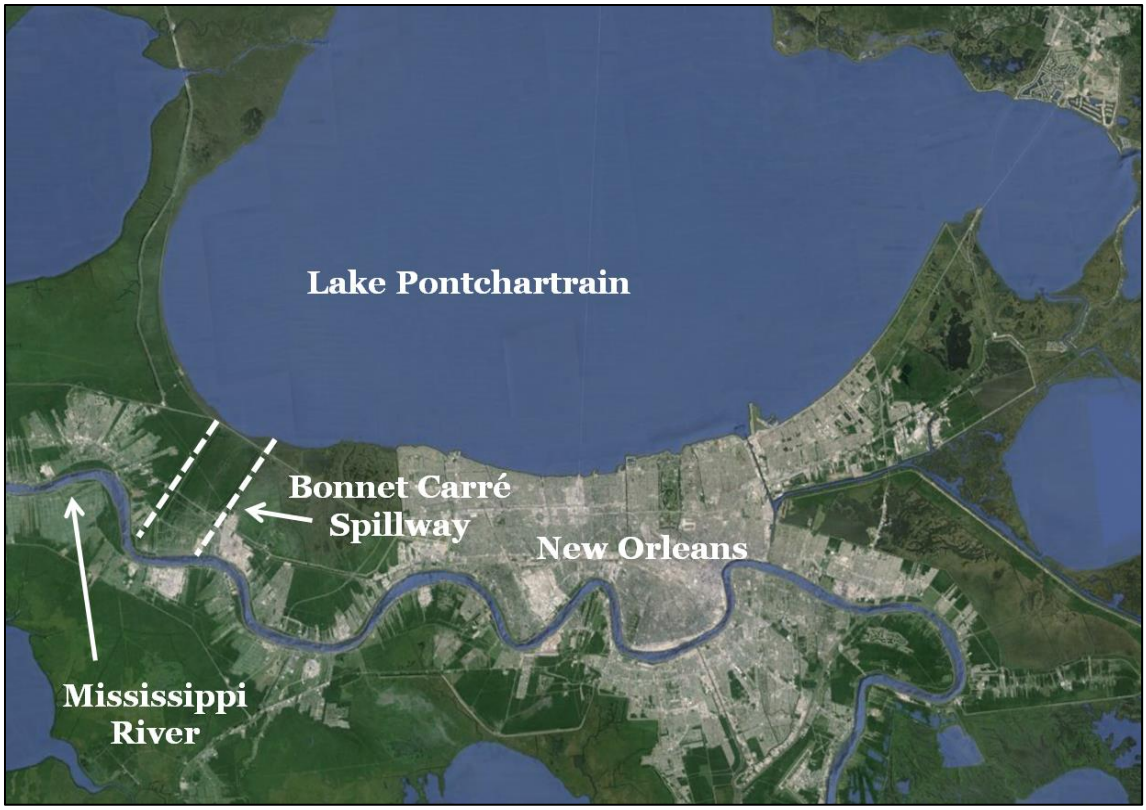

Figure 1.2. Map of the southern Lake Pontchartrain estuary. The locations of the Mississippi River, the Bonnet Carré Spillway diversion, and the city of New Orleans are shown. Lake Borgne is connected to the LPE via the Chef Menteur Pass and the Rigolets. (Source: Google Earth)

The opening of the BCS provides a flood release valve for the Mississippi River protecting the downstream city of New Orleans, LA, a highly industrial and populated area. The BCS is 31 km^2, located approximately 33 miles upstream the city of New Orleans and positioned at the edge of the southwest region of Lake Pontchartrain (Fig. 1.2). The 9.7 km long BCS was completed in 1931, allowing a direct flow path of flood water to enter Lake Pontchartrain and eventually into the Gulf of Mexico, bypassing New Orleans. The design capacity of the BCS is 7,080 $m^3 s^{-1}$ when the Mississippi river reaches the flood stage of 5.2 m (USACE, 2011).

Figure 1.3. The Bonnet Carré Spillway structure with two cranes pulling the pin-like timbers to allow water flow from the Mississippi River into the Lake Pontchartrain Estuary. (USACE, 2011).

The BCS consists of two control structures: a 2.4 km wide opening on the eastern side of the MSR and a 3.8 km wide opening of the southwestern side of Lake Pontchartrain. The main structure at the river consists of 350 bays which are blocked by one foot wide treated timber pins. A two crane system can open the BCS by manually lifting these wooden pins, allowing water to flow through the main channel of the spillway towards the LPE (Fig. 1.3).

During the BCS opening, the discharged floodwater significant changes the lake hydrodynamics. The floodwaters from the BCS, flows the shortest path eastward along the Lake Pontchartrain Estuary (LPE) southern border towards the Gulf of Mexico and gradually expand northward, distributing rich floodwater throughout the Lake (Chao et al., 2010).

Table 1.1. Operation of the Bonnet Carré Spillway since construction in 1932. All 10 BCS opening events are listed with the maximum flow capacity and the total water discharged.

Flood Event (year)	Number of Days Opened	Number of Bays Opened	Maximum flow capacity ($m^3 s^{-1}$)	Total water discharged (km^3)
1937	48	285	5,976	15.2
1945	57	350	9,006	30.1
1950	38	350	6,457	13.4
1973	75	350	5,862	23.5
1975	13	225	3,115	2.11
1979	45	350	6,457	13.9
1983	35	350	7,590	15.2
1997	31	298	6,882	11.7
2008	27	160	4,531	7.47
2011	42	330	8,947	21.9

*US Army Corp of Engineers, New Orleans District. Adapted after the Post-Flood Report.

In addition of the effects of the tides and winds, the stronger currents are found in areas that are shallow along the shoreline and the weaker current is near the lake's center (Chao et al., 2010; Signell et al., 1997). The spillway opening event also discharges high sediment loads into Lake Pontchartrain that can alter the shape and structure of the Louisiana coast (Fig. 1.4 a,b,c.).

The BCS had been opened 10 times since 1937, with the 3 more recent openings occurred in 1997, 2008, and 2011 (Table 1.1). During the 1997 BCS opening, the total volume of sediment rich floodwater was estimated at 1.18×10^{10} m^3, or twice the volume of the Lake (Turner et al., 1999). The total amount of sediment entering the lake in the 1997 BCS operation was about 9.1 Mt (Million Tons), more than 11 times as much as the normal yearly average (0.77 Mt) sediment loads to the Lake (Manhein and Hayes, 2002). The BCS was opened for 31 days in 1997 and load an average of 0.42 cm thickness of sediments over the entire Lake Pontchartrain area (Austin, 1997). Preliminary data suggest that over 1.23 Mt of sediment were loaded to the lake during the 2008 spillway opening (Fabre et al., 2012). The 2011 BCS opening yielded a thicker ~0.6 cm layer of fine grained sediment that covered the LPE area over a 42 days opening period (Fabre et al., 2013).

The openings also dramatically alter the distributions and dynamics of suspended sediments, salinity, and nutrients in the estuary. During these events, the fresh water dominates much of the lake and salinity is reduced significantly. The last three BCS opening occurred in 1997, 2008, and 2011. In 1997, 11.7 km^3 of flood water discharged into the LPE bringing 0.71 Mt of sediments (Table 1.2).

A.

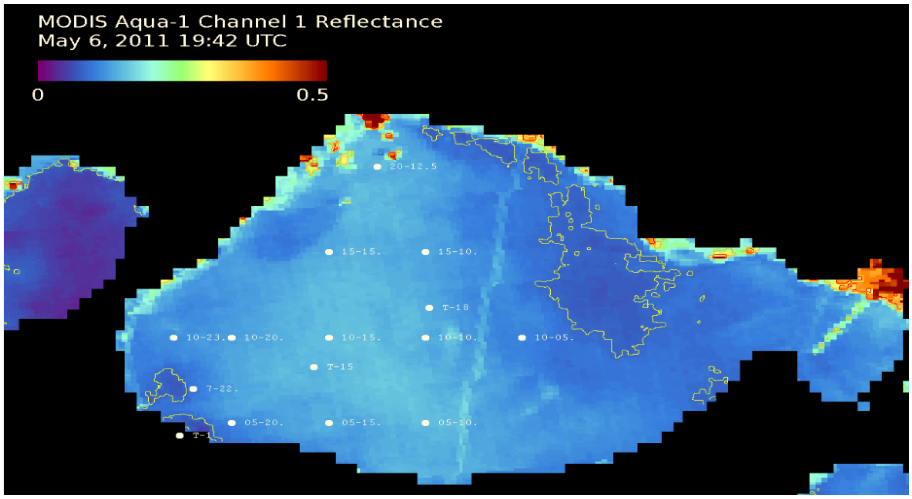

B.

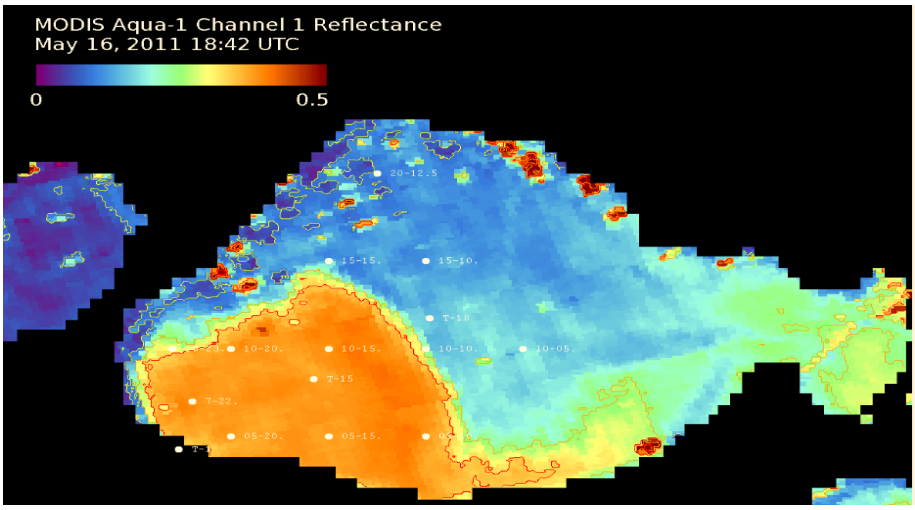

C.

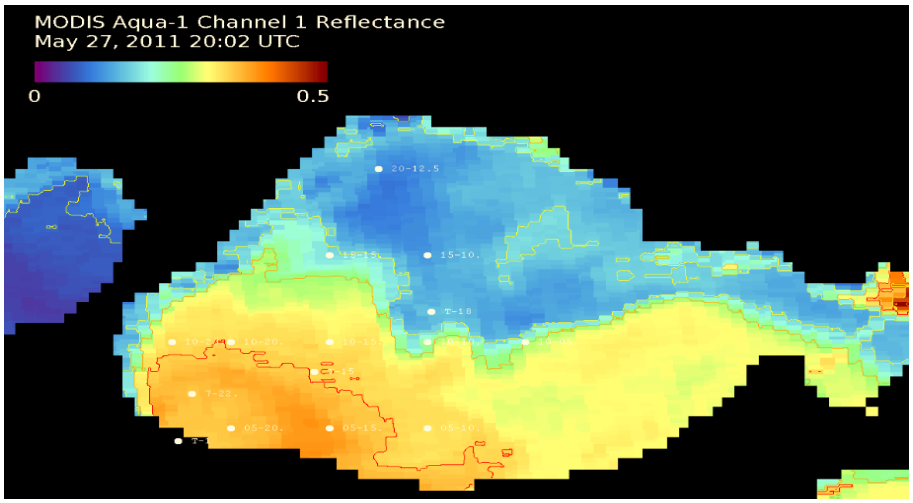

Figure 1.4 a,b,c. MODIS Aqua Reflectance of the sediment rich floodwater inputted due to the opening of the BCS. A) 3 days before the BCS opening B) 8 days after the BCS opened C) 20 days after the BCS opened in 2011.

In the 2008 BCS opening, the sediment loading increased to 1.23 Mt while discharged 7.5 km^3 of floodwater (Roy et al. 2013). The 2011 BCS opening was the largest of the three, adding 2.45 Mt of sediment mass and displaced 21.9 km^3 (~3 times the volume of Lake Pontchartrain) of floodwater in the LPE (Roy et al., 2013). Along with the heavy volume of floodwater, ~3.5 of the lake volume, the BCS opening also brought in ~26,000 Mg (Mega grams) of dissolved inorganic nitrogen and 1,122 Mg of dissolved inorganic phosphorus (Roy et al., 2013). The sediment, including nutrients and metals, from Mississippi River could potentially cause environmental problems. Large harmful algal blooms have occurred following previous BCS closures due to the increase of nutrient. These toxins blooms not only produced high levels of heptatoxins but also could cause another expression of eutrophication, a decrease in dissolved oxygen concentrations in the lake (Dortch et al., 1998).

Table 1.2. Three most recent Bonnet Carré Spillway openings with the amount of hydraulic and sediment loading. The total dissolved inorganic nutrients loading include dissolved inorganic nitrogen and dissolved inorganic phosphorus. (*Roy et al., 2013)

Opening Years	Hydraulic Load (km^3)	Sediment Load (million ton)	Total Dissolved Inorganic Nutrient Load (Mg)
1997	11.7	0.71*	15,299 DIN 584 DIP
2008	7.5	1.23*	9,938 DIN 374 DIP
2011	21.9	2.45*	26,085 DIN 1,122 DIP

*USGS: Lake Pontchartrain Basin (1998)

Eutrophication often occurs when there is an increase in nutrient concentration in the water column that is commonly due to anthropogenic pollution from municipal and agricultural runoff. Eutrophication can lead to dangerous algal blooms that began to decay which used up the dissolved oxygen in the water, creating hypoxic conditions.

Without sufficient amount of dissolved oxygen in the waters; large numbers of microorganisms and aquatic organisms will not survive (Peters, 1986). Due to the increase of nutrients from the incoming sediment of the BCS operations, eutrophication can be a factor that affects the LPE water quality.

1.3 Phosphorus and Internal P Loading

Phosphorus (P) and nitrogen (N) are the primary nutrients that cause eutrophication. Phosphorus is typically a limiting nutrient in freshwater systems while nitrogen limits algae growth in most saline systems. The excess runoff of P from agriculture leads to a buildup of P concentration in the sediments of downstream aquatic systems that can contribute to water quality degradation.

P in the sediment exists in organic forms or inorganic forms. In neutral to alkaline sediments, the dominant form is calcium-bound P, while in acidic soils, P is bound to iron and aluminum oxides. Both of these forms of P have extremely low solubility so very little P is lost by leaching due to the strong affinity to P by iron and aluminum in the sediment particles. Most P losses occur as P is removed by plant uptake and microorganism consumption. The low concentration and immobility of P in the soil solution are due to the low solubility of P and the retention of P on the surfaces of sediment particles. The solubility and fixation of inorganic P compounds are controlled by the precipitation of iron, aluminum, calcium, and magnesium phosphate compounds. The solubility of the P in the newly precipitates is much greater than in older precipitates. Under anaerobic conditions, the reduction of ferric iron to ferrous iron allows P to become more soluble reactive.

When P is added to sediments, P sorption occurs. Phosphorus sorption can be a fast surface or slow reaction of P on solid phase (soil minerals and organic compounds). Sorption of P initially proceeds by a rapid exothermic ligand exchange reaction with the reactive surface groups. Phosphate surface complex can form when a hydroxyl or water molecule is released from the surface (Frossard et al., 1995). A slow reaction occurs by ion exchange with exchangeable cations or cations in crystal lattices. Phosphorus sorption in this context also includes "adsorption" and "retention". The sorption process is controlled by the concentration of P in the water column and the ability of solid phase to replenish P into solution (capacity). When inorganic P is added to soil, sorption reactions proceed until a new equilibrium is reached.

Sediments in an estuarine system may act as either sinks or sources of P. Upland soils are eroded by water and then deposited in downstream sediments. Sediments are often a major contributor of P to water, but may also act as a sink to trap P from water. Sharpley et al. (1981) found that an increase of sediment concentration in runoff decreased the amount of soluble P concentration. One major internal P flux in a lake system comes from the release of P in the sediment by diffusion (Jensen and Anderson, 1992). To determine the P movement in the sediments, a P desorption index called the equilibrium phosphorus concentration (EPC) is measured (Haggard and Sharpley, 2007). The EPC in the sediments is compared with the dissolved P concentration in water column. If EPC is greater than dissolved P in water, sediments will behave as a source by releasing P to water until a new equilibrium is reached. If EPC is less than dissolved P in water, soils or sediments will adsorb P from water, thus decreasing P concentration in water.

1.4 Phosphorus Fractionation

Phosphorus fractionation schemes have been used to study soils and sediments for over 50 years. Phosphorus is an essential nutrient that promotes growth and controls the water quality of a system. The environment contains various forms of P, including bioavailable, organic bound, inorganic bound and residual P. Phosphorus fractionation is regulated by the chemical and physical properties and also the redox conditions of the environment.

Phosphorus fractionation can determine the amount of P in each pool using series of reactants to extract or isolate P. Each P fractionation scheme is useful for different types of soils and sediments, but there are limitations for each method. Pretreatment of samples before the fractionation method can change the composition of the sediment and cause a different result from original sample (Reddy and Delaune, 2008).

Several additional sediment analyses can be performed in conjunction with core incubations to provide information that is useful in interpreting sediment P release results. The top 5 or 10 cm of sediment can be extruded from cores for analysis of sediment total P; porewater dissolved inorganic P, sequential P fractionation, and metals. An example of sequential P fractionation that can be useful in internal loading studies involves determining the amount of P bound to 1) aluminum (Al-P) or iron (Fe-P), which represents a redox insensitive (Al-P) and a redox-sensitive (Fe-P) mineral association that can become soluble under anoxic conditions, and 2) calcium (Ca-P) or magnesium (Mg-P), which are both more stable mineral associations. Further, sediment Fe:P ratios can be calculated to provide insight on the potential P-binding capacity of sediments. Iron-rich

sediments that remain oxidized have been shown to release very little P when Fe:P ratios are above 15 (by weight) (Ogdahl et al., 2014).

CHAPTER TWO: EFFECTS OF THE 2011 BONNET CARRÉ SPILLWAY OPENING ON SEDIMENT PROPERTIES AND PHOSPHORUS FORMS IN THE LAKE PONTCHARTRAIN ESTUARY

2.1 Introduction

The Mississippi River Basin is a highly engineered system comprised of levees and flood control structures along its 3,766 km route. There are now approximately 8,000 dams, diversions, and spillways systems along the continuous system of levees along the Mississippi River system to protect low-lying area from floods (Blum and Roberts, 2009). These control structures help protect southern Louisiana and the city of New Orleans from annual summertime flooding and allow permanent settlement along the river. The Bonnet Carré Spillway (BCS) was constructed in 1931 in response to the Great Mississippi flood of 1927 to serve as a controlled flood release valve for the Mississippi River (USACE, 2012). The 10 km long BCS consists of 350 bays capable of diverting up to 7,080 $m^3 s^{-1}$ (250,000 $ft^3 s^{-1}$) of the Mississippi River floodwater into Lake Pontchartrain in order to protect the downstream city of New Orleans (USACE, 2012). Since construction, the BCS has been opened ten times, most recently in the early summer of 2011 (Roy et al., 2013).

These openings allow large amount of suspended sediment rich water comprised of ~ 10 % sand and ~ 90 % mud, into the Lake Pontchartrain Estuary (LPE), eventually draining into the Gulf of Mexico (Allison and Meselhe, 2010). An average of more than 7,080 $m^3 s^{-1}$ with the maximum of ~ 17 % of the Mississippi River freshwater flood stage volume entered the Lake in 2011 (Roy et al., 2013; Nittrouer et al., 2012).

Monitoring during the 2011 BCS opening determined that the river plume deposited approximately 2.45 ± 1.35 Mt of sediment throughout the Lake (Fabre et. al, 2012). Approximately 10-15 % of the upper layer of river water entered the LPE carrying 31 to 46 % of the sand suspended sediment load carried by the Mississippi River (Nittrouer et al., 2012). The majority of the sand particles settled within the spillway and near the discharge outlet into Lake Pontchartrain, while the lighter mud (clay and silt) particles remain suspended in the water column longer due to the energetic flow. The high sediment retention rates into a semi-enclosed estuarine basin can change the trophic status of the Lake if the associated particulate phosphorus (P) load is eventually mobilized and reintroduced back into the water column.

Opening of these large river diversions can discharge substantial volumes of floodwater, often greater than the entire volume of the LPE. Increased nutrient rich water greatly increases the bioavailability of nutrients in the LPE (McCorquodale et al., 2009; Turner et al., 2002). During diversions openings, phosphorus limits phytoplankton growth in the LPE due to the high molar N: P ratio (~ 50), a consequence of the high nitrate loading from the inflowing Mississippi River (Roy et al., 2012). After the diversion events, N-limitation returns as the sediments provide an internal source of P to the water column (Roy et al., 2013). Phosphorus availability is an important factor in the growth of N-fixing harmful algae during these low N-limited conditions. However, our knowledge about the role of the internal sediment P loading on surface-water P enrichment in lake systems is rather limited (Pant and Reddy, 2001; Reddy et al., 2007).

Lake sediments can function as a source or sink for dissolved nutrients on the overlying water column. The concentrations of P in the water column can affect the release of P from the sediments. The physical and chemical reactions of P between the water and sediment layer in natural systems include adsorption/desorption with the sediment particle and oxidation-reduction conditions between sediment water layers, which regulate soluble P concentrations in estuaries. Sediments rich in P tend to release P when concentrations are low in the water column. Conversely, water columns with high concentration of P tend to lose P to the sediment (Reddy and DeLaune, 2008). Previous research indicates that internal loading of P from sediments by diffusion accounts for ~ 517 Mt y^{-1} of dissolved inorganic P (DIP) (Roy et al., 2012), a comparable amount to that loaded by the BCS opening in 2008.

2.2 Phosphorus Forms: Organic and Inorganic P

Phosphorus can be present in two major forms, organic and inorganic, in the sediment and the water column. The largest pool of P tends to be in the particulate inorganic form in estuarine systems (Reddy et al., 2008). Inorganic P compounds in the sediment can be composed of calcium and magnesium as well as iron and aluminum dependent upon source material, pH and redox (Reddy et al., 2011). Soluble inorganic P is released through dissociation of inorganic minerals and the mineralization of organic material. This form of P is readily available to be taken up by plants and algae. Soluble P generally makes up the smallest component of total P in sediments. Large amounts of the sediment's P content is sorbed to compounds that are created when the negatively charged ions of dissolved P binds to cations and metals such as aluminum, iron,

magnesium and calcium on clay particles (Reddy and DeLaune, 2008). The organic P in the sediment is formed primarily from decomposed plant (algae or macrophyte) or animal tissue and is contributed through biological processes to form organic materials. Organic P forms in estuary systems include: inositol phosphate associated with humic and fulvic acid complex, phospholipids and nucleic acids (Turner et al., 2006). Organic P (Po) forms can be convened into 2 groups; easily decomposable Po (nucleic acids, phospholipids, and sugar phosphates) and slowly decomposable Po (inositol phosphate or phytin) (Reddy et al., 2011). Some of these forms are considered very stable in anaerobic environments and therefore lead to long term organic P sequestrations in estuarine systems.

The rate of P availability depends on the solubility of P and the binding strength of the surface of the particle. Phosphorus chemistry in soils and sediments is greatly influenced by the oxidation-reduction status (redox potential). Under oxidized conditions, presence of ferric and manganic oxides and hydroxides allow for significant adsorption sites for P. In addition, ferric and manganic phosphate minerals can form and are stable under oxidized conditions. But under reducing conditions, these minerals are highly unstable, resulting in dissolution and release of soluble P into the pore water and eventually to the water column (Patrick et al., 1973; Moore and Reddy, 1994).

The goal of this chapter was to investigate changes in the sediment P pools for Lake Pontchartrain sediments before and after the 2011 BCS opening by (1) measuring the total phosphorus (TP) of the lake's sediment, and (2) determining the percentage of various inorganic and organic forms of P from the 0-5 cm and 5-10 cm depth intervals.

2.3 Materials and Methods

2.3.1 Site Study

Lake Pontchartrain is a shallow, oligohaline estuary located in southeastern Louisiana, U.S. with dimensions of 64 km in east-west width by 39 km in north-south width (1,634 km^2 surface area) and a mean water depth of 3.7 m (Turner et al., 2002).

Figure 2.1. Map of the Lake Pontchartrain estuary. The locations of the Mississippi River, the Bonnet Carré Spillway diversion, and the city of New Orleans are shown. Lake Borgne is connected to the Lake Pontchartrain estuary via the Chef Menteur Pass and the Rigolets. (Source: Google Earth)

The Lake is connected to the Rigolets and Chef Menteur Pass on the eastern side of the Lake, which allow exchange with the Gulf of Mexico (Fig. 2.1). The average surface wind speed is 7.5 m s^{-1} and the current speed is 10 cm s^{-1} in Lake Pontchartrain (Signell and List, 1997). The salinity of the Lake typically ranges from 2 to 9 PSU, depending on the influences of saltwater intrusion from the Gulf of Mexico and freshwater tributaries inflow from the northern watershed and Lake Maurepas on the western side (Li et al., 2008). The salinity of the estuary can be dramatically altered by influx of Mississippi River floodwater when the BCS is opened. The water column of LPE is generally well oxygenated, with dissolved oxygen >>2 mg L^{-1}, due to its shallow depth and constant mixing by surface winds.

2.3.2 Sampling and Sediment Characteristics

Sediment cores were collected from 15 stations using a piston corer in the Lake on May 8, 2011, one day before the opening of the BCS, and July 7, 2011, 17 days after the closure of BCS (Fig. 2.2). Field measurements of dissolved oxygen, temperature, and secchi disk depth were also taken during both field sampling events. Cores were sectioned into 0-5 cm and 5-10 cm intervals immediately after return from the field for sediment characterization which included moisture content, bulk density, loss on ignition, total carbon (C), total nitrogen (N), total P, total metals, and sediment grain size. Fabre et al. (2013) reported that the "average" flood deposit thickness in the Lake was ~0.6 cm. Assuming even distribution in the entire LPE, the 0-5 cm sections would represent a mixture of thin flood layer on top (0-0.6 cm) and pre-2011 sediment (0.6-5 cm). Of course sediment accumulation in the Lake might be highly localized, being high near the outlet of BCS and small far from this outlet.

The total net weight was measured for each sediment interval. Moisture content of each sediment sample was determined by placing a homogenized sample in a forced air drying oven at 70º C until constant weight. Bulk density was determined on a dry weight basis.

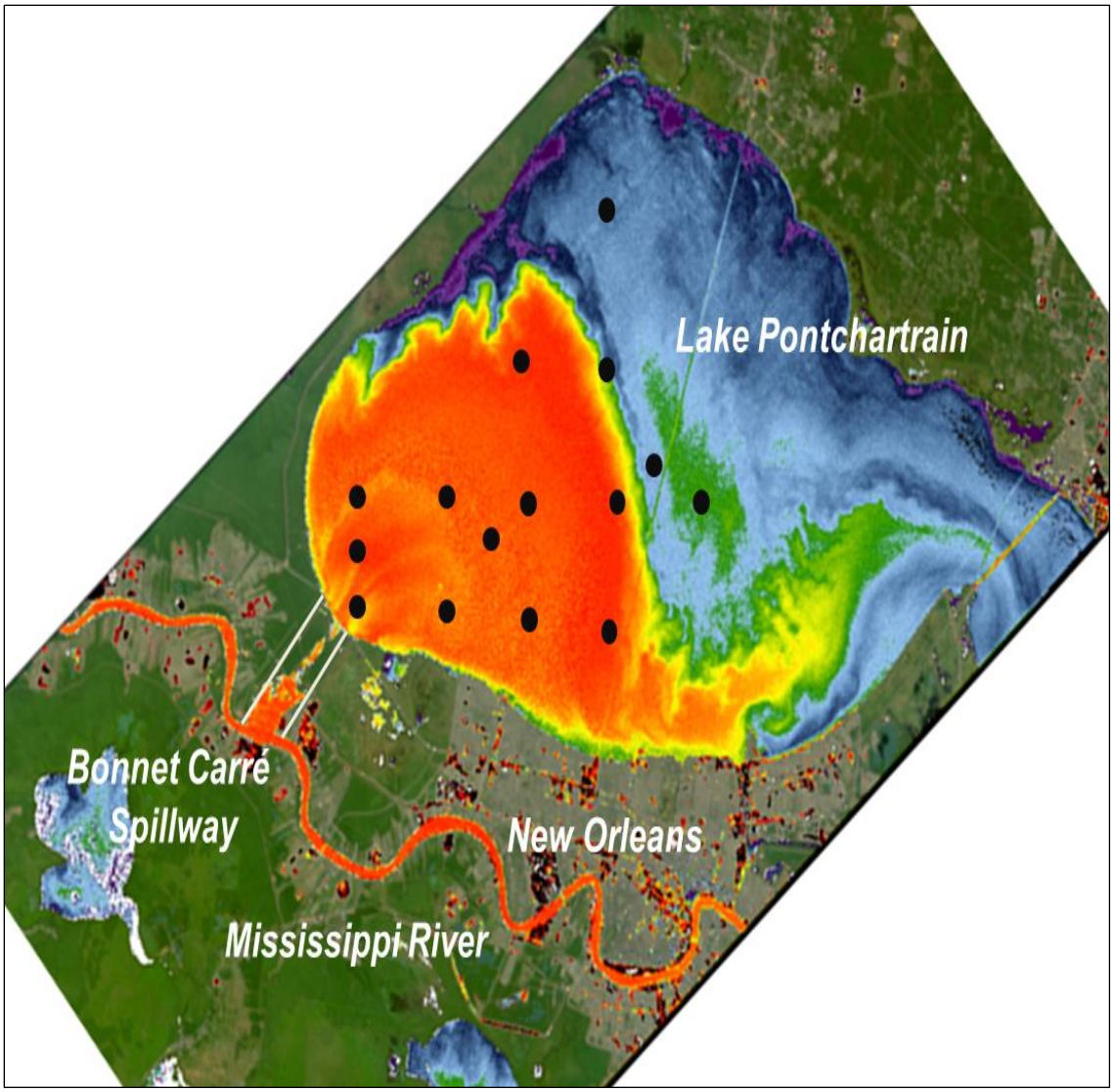

Figure 2.2. False color imaging areal map of the Lake Pontchartrain estuary. The locations of Mississippi River and the Bonnet Carré Spillway are shown. The sampling locations are represented by the dots. Suspended sediment concentrations are represented in the red plume at 547nm reflectance. (Naval Research Laboratory, Stennis Space Center, MS)

Loss on ignition was measured by placing the dried, ground sediment subsample into a 550°C muffle furnace for 4 h to remove the organic matter. The difference in weight before and after the ashing determined the weight percent organic matter. Dried, ground sediment subsamples were also analyzed for total C and N using an Elemental Combustion System with a detection limit of 0.005 g kg^{-1} (Costech Analytical Technologies. Inc., Valencia, CA). Field moist sediment samples were used for grain size analysis using a Beckman-Coulter laser particle size analyzer (Model LS 13 320). A subsample was mixed with at least 50 ml of 30 % hydrogen peroxide to oxidize all organic matter in the sample. The solution was then centrifuged and decanted to remove any residual hydrogen peroxide and placed on a longitudinal shaker to ensure all aggregates were broken apart. The detection grain size range for the particle size analyzer is from 0.02 to 2000 µm.

2.3.3 Total Phosphorus- [TP] and Metal Analysis

A 0.3 g dried ground sediment sample was weighed in a 50 ml glass beaker and placed into a 550°C muffle furnace for 4 hours to burn off all organic materials. After cooling, 20 ml of 6 M hydrochloric acid (HCl) was added and the sample was heated on a hot plate at 130°C for 5 hours, dissolving all the inorganic forms of P contained within minerals remaining in the sediment sample (Anderson, 1976). The solution was then filtered using a Whatman #42 filter and diluted in a 50 ml volumetric flask. The dilutant was run for TP on the Seal Analytical AQ2 discrete colorimetric analyzer (method 365.1; USEPA, 1993).

Metals concentration of sediment samples were measured using a method after Malecki-Brown and White (2009). An approximately 0.5 g dried ground sample was placed in a 50 ml beaker and ashed at 550˚C for 4 h. A 20 ml 6 M HCl was added into the sample beaker and placed on a 120˚C hot plate for 5 h to dissolve all of the metals. The digested sample was then filtered through a Whatman #42 filter paper and diluted in a 50 ml volumetric flask using deionized water. The filtrate is then analyzed on a Varian model inductively coupled plasma elemental analyzer (MPX ICP-OES).

2.3.4 Phosphorus Fractionations

A sequential P fractionation extraction method was also utilized on field moist sediment samples. The fractionation scheme included five sequential extractions that determine the readily available P, alkali extractable organic P, iron/aluminum-bound P, calcium/magnesium-bound P, and residual P summing to the total P in the sediments. Chemical fractionation schemes are used to estimate the labile and nonlabile P pools in the sediment (Reddy et al., 1998; Reynolds and Davis, 2001). Concentrations of P pools in sediments depend on the concentrations in the lake water, the concentration of soluble phosphate between the pore water, and the solid component in the sediment. Adsorption/desorption mechanisms and biological uptake can also have a great impact. Due to the differences in the origin and genesis of water bodies, as well as a large number of external and internal factors, the biogeochemical cycling of P fractions can vary greatly.

The order of the fractions corresponds to availability or potential for release from highest to lowest. Sediment total P values can also be used to determine locations (e.g.,

near tributary outflows) where there has been significant external loading of P in the past, leading to enrichment of the sediment (McCorquodale et al., 2009). Since iron and manganese phosphate mineral formation is controlled by the redox potential of the sediment, it is important that sediment samples were collected under reduced conditions and handled appropriately during P fractionation to get an accurate picture of the P status. A 1-2 g field-moist sediment sample was weighed and placed into a 50 mL centrifuge tube and sequentially treated with the following extractants (Fig. 2.3).

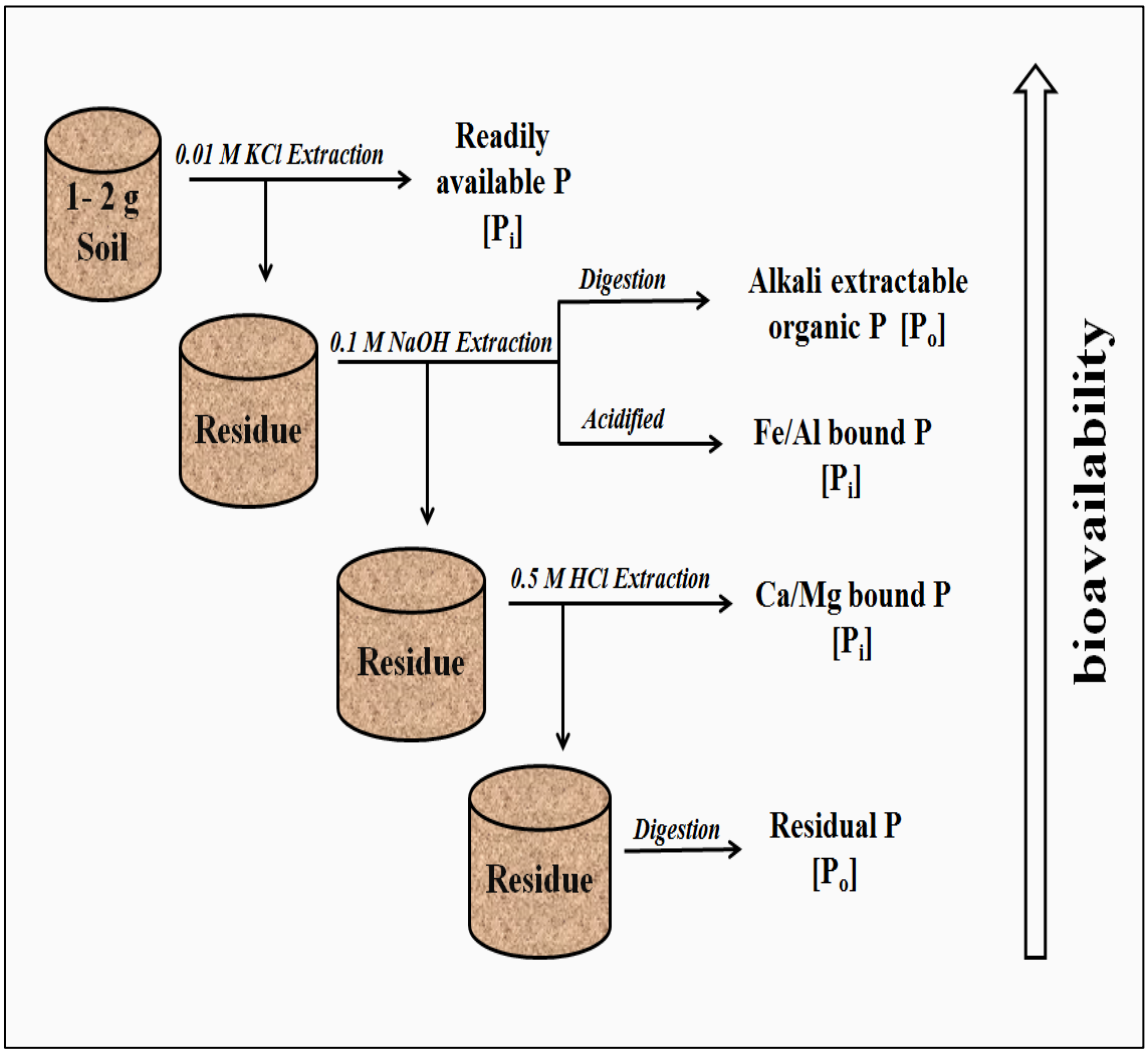

Figure 2.3. Phosphorus sequential extraction scheme according to the bioavailability of P.

KCl-extractions- [Pi]

Weighed wet sediment samples were extracted with 20 ml of 0.01 M potassium chloride (KCl) solution. Sediment suspensions were equilibrated for a period of 1 h by continuously shaking on an longitudinal shaker at room temperature, followed by centrifugation at 5212 g for 10 min. Supernatant solutions were filtered through 0.45 μm membrane filters. Solutions were then analyzed for DIP (USEPA, Method 365.1, 1993). The supernatant represents the readily available form of P in the water pool (water soluble plus exchangeable pool). The tubes were weighted after each filtration to be corrected for each solution gained or lost between each extraction. The residual sediment sample remaining in the centrifuge tube was then used in the following sequential extraction scheme.

NaOH-extractions- [NaOH-Pi]

The residual sediment obtained from the KCl extraction was treated with 20 ml of 0.1 M NaOH. Sediment suspensions were equilibrated for a period of 17 h by continuously shaking on a longitudinal shaker at room temperature, followed by centrifugation at 5,212 g for 10 min. The supernatant solution was filtered through a 0.45 μm membrane filter and was analyzed for DIP. Sodium hydroxide ($NaOH\text{-}P_i$) represents the iron and aluminum bound P. Extraction with 0.1 M NaOH also remove P associated with humic and fulvic acids. The residual solution was used in the next sequential extraction.

A subsample of NaOH [Pi] aliquot was digested to obtain the TP of the extracted NaOH-Pi sample. In a digestion tube, 5 ml of NaOH extractant, 1 ml of 11 M H_2SO_4, and ~ 0.35 g of potassium persulfate was added. The tube was placed on the digestion block at 150°C for 3 to 4 h to remove all excess water from the sample. The remaining aliquot solution was further digested on the digestion block for 3 to 4 h at 380º C with a glass funnel to inhibit any sample evaporating from the digestion tube. After the digestion, the samples were diluted with 10 ml deionized water and vortex to evenly mix the solution. The samples were analyzed for TP (USEPA, Method 365.1, 1993). The difference of NaOH-TP and NaOH-Pi was the NaOH-Po which was P that was associated with the organic P bound to alkali metals found in the sediment (Eq. 2.1).

Equation 2.1: $\text{NaOH [TP]} = \text{NaOH [P}_i\text{]} + \text{NaOH [P}_o\text{]}$

HCl-Extractions- [HCl-Pi]

Twenty ml of 0.5 M HCl was added to the residual sediment from after the NaOH extraction. Sediment solutions were allowed to equilibrate for a period of 24 h by continuously shaking on an automatic shaker at room temperature, followed by centrifugation at 5,212 *g* for 10 min. The supernatant solution was filtered through a 0.45 μm membrane filter and the residual sediment was then used for the residual P extraction. Filtered solutions were analyzed for DIP (USEPA, Method 365.1, 1993). This fraction of HCl-Pi represents the calcium and magnesium bound P. The P extracted with an acid represent the P tied up in apatite minerals, essentially as calcium phosphate. The P can also be present in transitional forms of calcium, such as monocalcium, dicalcium and octa-calcium phosphate (Reddy and Delaune, 2008). Apatite P is not readily for algae to

uptake and is particularly stable under normal environmental conditions. Only very acidic conditions can significantly mobilize this P pool through the production of organic acids or other modifications which lower the pH.

Residual- [Res-TP]

The Residual P fraction represents both the refractory organic P and any other mineral P fractions that are not extracted with KCl, NaOH, or HCl reagents from the previous extractions. The remaining residual sample from the extraction was transferred into a 50 ml beaker and placed in a drying oven at 70ºC for two days or until the weight was constant. The total phosphorus ashing-digestion method was then performed and analyzed using the TP method (USEPA 365.1; 1993).

2.4 Results and Discussion

Beside moisture content and bulk density, the physical sediment characteristics are consistent between the 0-5 cm and 5-10 cm sediment interval. The sediment depths of 0-5 cm and 5-10 cm have a fairly consistent material makeup. This may be due to strong incoming flow of flood water from the BCS. The disturbance from the waves also constantly mixes the surface sediment layer of the shallow Lake (Flocks et al., 2010). The average moisture content before the opening was 63 ± 10 % from the 0-5 cm segment intervals and 58 ± 10 % in the 5-10 cm segment intervals. The higher moisture content at the surface 0-5 cm segment was due to the close proximity of the sediment and water interface. After the closure of the BCS, the moisture content was 68 ± 9 % and 62 ± 9 % in 0-5 and 5-10 cm segments, respectively (Table 2.1).

The average bulk density before the BCS opening was 0.52 ± 0.18 g cm^{-3} in 0-5 cm segment interval and 0.61 ± 0.22 g cm^{-3} in 5-10 cm segment interval. The average bulk density after the BCS event was not significantly different at 0.53 ± 0.2 g cm^{-3} and

Table 2.1. Sediment characteristics and mean ± 1 standard deviation from the 0-5 cm and 5-10 cm segment intervals before and after the 2011 Bonnet Carré Spillway opening. Student's T tests were used to test significance at $\alpha < 0.05$. The asterisks represent significance between pre-opening and post-closure of the spillway.

	0-5 cm Sediment Intervals		5-10 cm Sediment Intervals	
	Pre-Opening	Post-Closure	Pre-Opening	Post-Closure
Moisture Content (%)	0.63 ± 0.10 *	0.68 ± 0.09 *	0.58 ± 0.10	0.62 ± 0.09
Bulk Density (g cm^{-3})	0.52 ± 0.18	0.53 ± 0.20	0.61 ± 0.22	0.68 ± 0.22
Loss of Ignition (%)	7.15 ± 2.13	7.76 ± 1.59	6.75 ± 1.87	6.77 ± 1.82
Total P (mg kg^{-1})	525 ± 62.2 *	677 ± 44.3 *	515 ± 75.3 *	656 ± 42.2 *
Total N (mg kg^{-1})	0.18 ± 0.04 *	0.20 ± 0.04 *	0.15 ± 0.04	0.16 ± 0.04
Total C (mg kg^{-1})	1.45 ± 0.25 *	1.59 ± 0.25 *	1.43 ± 0.5	1.41 ± 0.28
Al (mg kg^{-1})	34,048 ± 10,727	36,378 ± 8,369	31,732 ± 8,831	34,719 ± 6,787
Fe (mg kg^{-1})	28,360 ± 6,501	30,268 ± 4,361	27,482 ± 5,629	29,965 ± 4,135
Ca (mg kg^{-1})	8,042 ± 4,332	6,226 ± 2,982	9,972 ± 6,959	7,873 ± 4,694
Mg (mg kg^{-1})	8,101 ± 1,758	8,648 ± 1,077	7,918 ± 1,535	8,698 ± 1,419

* $P < 0.05$

0.68 ± 0.22 g cm^{-3} in 0-5 cm and 5-10 cm sediment intervals, respectively. Sites along the western LPE, most proximal to the BCS, had a higher bulk density. This result can be expected as larger, heavier sand size particles do not remain suspended in the water column as water velocity slows as the plume entered the estuary. The average pre-opening loss on ignition (LOI) was 7.15 ± 2.13 % and 6.75 ± 1.87 % in 0-5 cm and 5-10 cm sediment interval, respectively. After the closure of the BCS, the average LOI was not significantly different at 7.76 ± 1.59 % and 6.77 ± 1.82 % from 0-5 cm and 5-10 cm segment intervals, respectively.

2.4.1 Grain Size Analysis

The grain size in the LPE at the 0-5 cm sediment interval consists of 23 % sand, 49 % silt, and 28 % clay before the BCS opening. The surface 0-5 cm grain size varies throughout the LPE, potentially as a result of tidal currents and wind induced mixing (Fig. 2.4). At the 5-10 cm sediment interval, the grain size was 21 % sand, 49 % silt, and 29 % clay before the BCS operation. After the closure of the BCS, the 0-5 cm sediment interval consists of 29 % sand, 44 % silt, and 26 % clay. At the 5-10 cm sediment interval, the grain size was 32 % sand, 43 % silt, and 27 % clay after the BCS operation. The majority of the heavier sand fraction was quickly deposited in the BCS while the finer sand and mud fraction entered the LPE (Fig. 2.5). Similar findings from the 1973 BCS opening which deposited a 19 cm thick layer of silty sand near the spillway's mouth (Crocker, 1988). During the 2011 BCS event, 2.6 Mt of sediment entered the BCS structure containing mostly fine sand (Allison et al., 2013).

The mean grain size for the 0-5 and 5-10 cm segment intervals was 6.22 φ (~ 13 μm) and 6.32 φ (~ 13 μm) before the BCS opening; after the closure of the BCS, the mean grain size significantly increase to 5.81 φ (~ 17 μm) and 5.75 φ (~ 19 μm) from the 0-5 cm and 5-10 cm segment intervals, respectively. Indicating that the sediment at pre-opening conditions were medium to fine silt, while after the BCS operation event were from medium to coarse silt. Overall, the grain sizes were very poorly sorted (sorting values range from 2.6 ϕ to 3 ϕ), while the skewness is near symmetrical (skewness value ranging from -0.03 to -0.07).

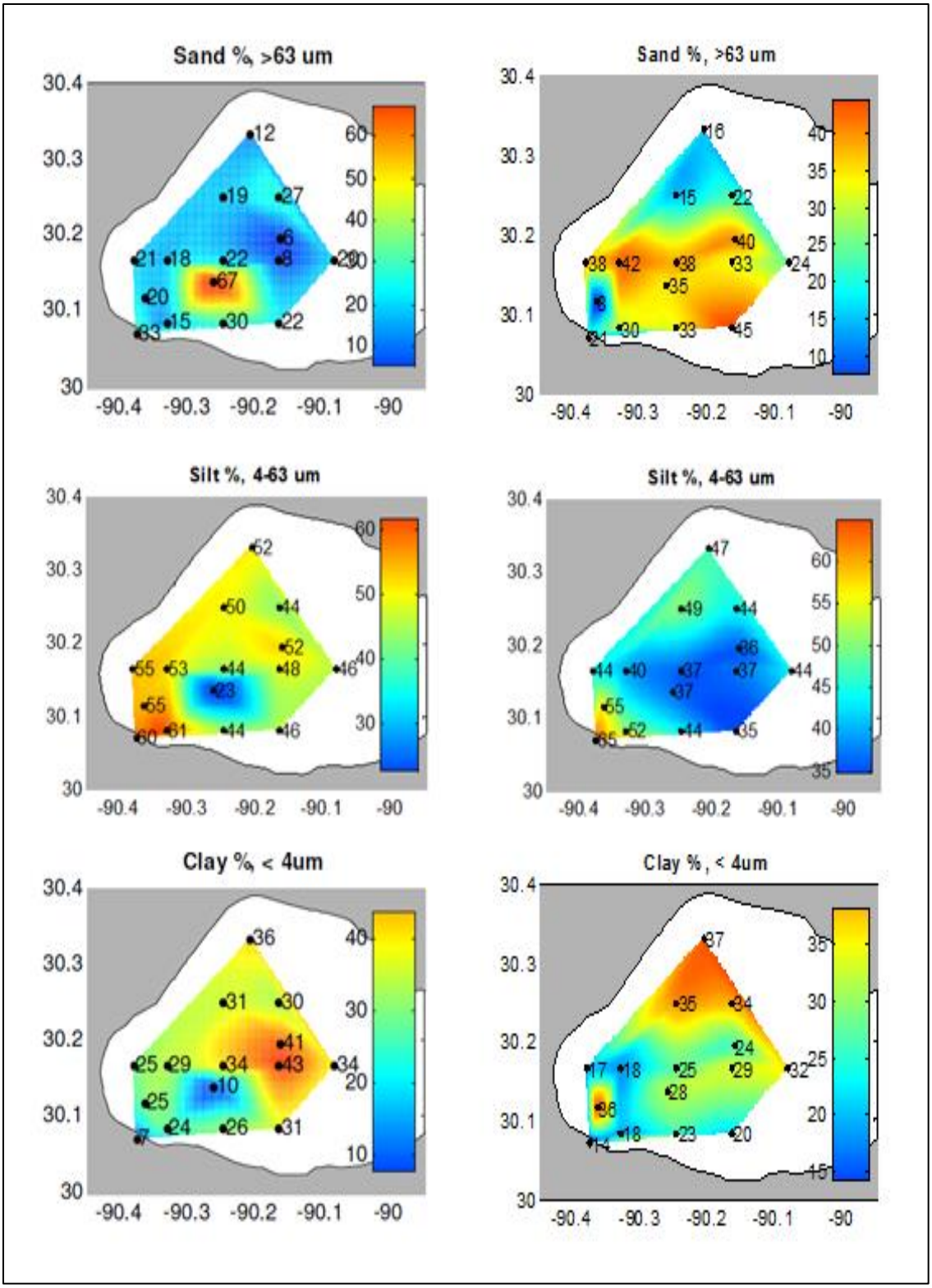

Figure 2.4. Grain size of sand, silt, and clay at each station from the 0-5 cm sediment interval for preopening (left) and post closure (right).

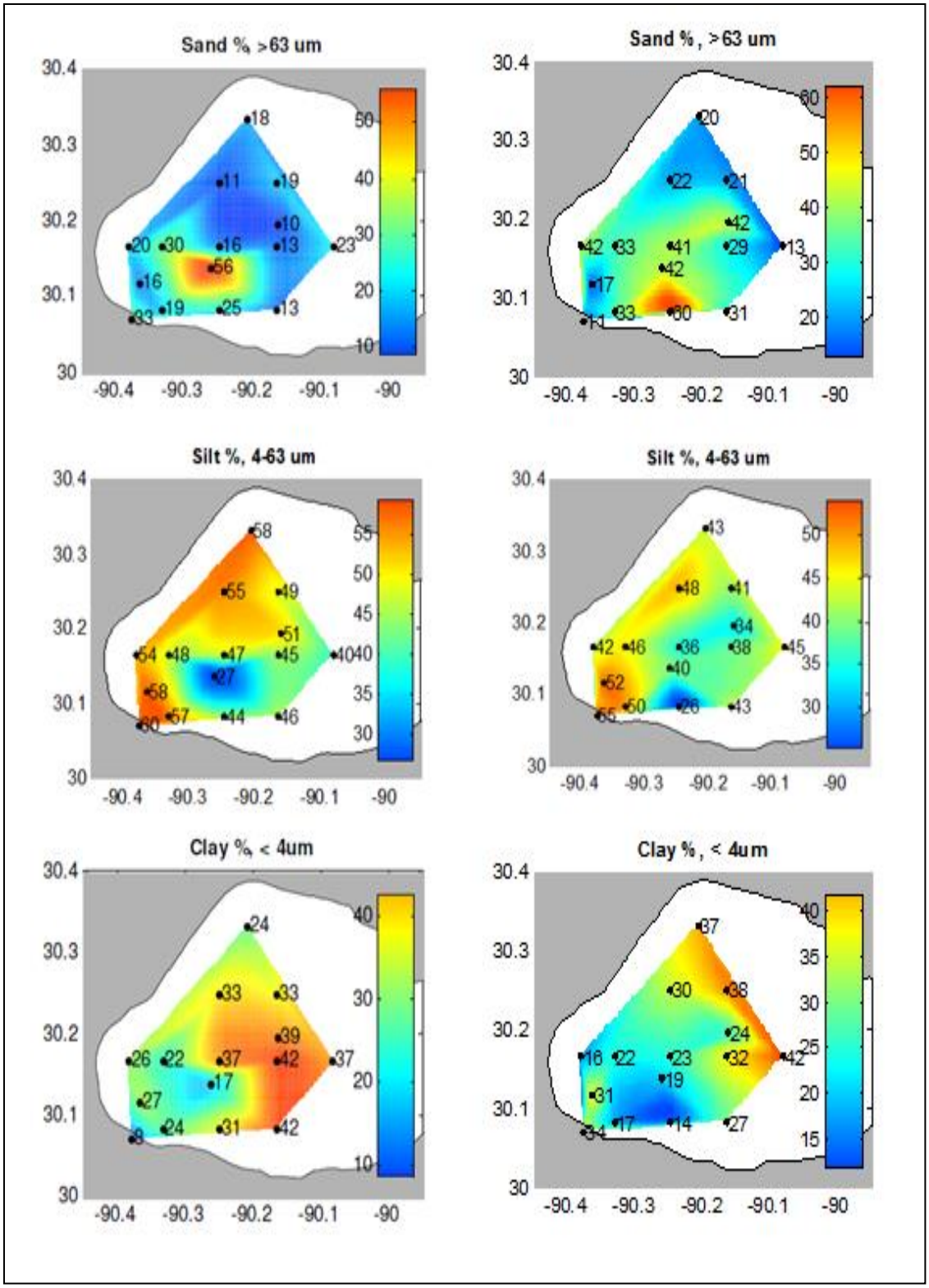

Figure 2.5. Grain size of sand, silt, and clay at each station from the 5-10 cm sediment interval for preopening (left) and post closure (right).

Correlations of the clay fraction of pre BCS opening with the distance from the BCS entrance into the LPE were $r^2 = 0.50$ and 0.37 at 0-5 and 5-10 cm segment interval, respectively. Inversely, the percentage of sand and silt decreases as distance increased from the BCS entrance to the LPE. Some sampling stations along the LPE have sandy pockets which could be artifacts of earlier dredging activities. In addition, a false signal that can increase the percentage of "coarser or fine sand" could be due to the presence of shell fragments in the sample.

The average sediment TP concentration before the opening was ~ 525 ± 62.2 mg kg^{-1} in 0-5 cm segment intervals and ~ 515 ± 75.3 mg kg^{-1} in 5-10 cm sediment intervals. After the closure of the BCS, the TP concentration was ~ 677 ± 44.3 mg kg^{-1} in the 0-5 cm sediment interval and ~ 656 ± 42.2 in the 5-10 cm; a significant increase of 27 % from 0-5 cm and 29 % from 5-10 cm segment intervals from the 2011 BCS opening event. The pre-opening TP concentrations from the 0-10 cm sediment interval gradually increases ($r^2 = 0.16$) comparing with the distance from the mouth of the BCS (Appendix F). After the 42 days BCS opening, the TP concentration from the 0-10 cm sediment interval is similar throughout the whole sampling area; suggesting that the newly added sediment is even distributed in the LPE sediment with constant mixing of the currents.

There were no significant differences in the metal concentrations before and after the 2011 BCS event using a paired t test. The concentration of aluminum (Al), iron (Fe), calcium (Ca), and magnesium (Mg) were ~ 34,048, ~ 28,359, ~ 8,041, and ~ 8,099 mg kg^{-1} in the 0-5 cm sediment interval before the opening, respectively. In the 5-10 cm sediment interval, the concentration of Al, Fe, Ca, and Mg were ~ 31,732, ~ 27,842, ~ 9,972, and ~ 7,918 mg kg^{-1} before the opening. After the closing of the BCS, the

concentration of Al, Fe, Ca, and Mg were ~ 36,378, ~ 30,267, ~ 6,226 mg kg^{-1}, and ~ 8,648 mg kg^{-1}in the 0-5 cm sediment interval. In the 5-10 cm sediment intervals, the concentration of Al, Fe, Ca, and Mg were ~ 34,719, ~ 29,965, ~ 7,873, and ~ 8,698 mg kg^{-1} after the closing of the BCS.

The total C and total N concentration before the BCS opening in the 0-5 cm segment interval were 1.45 ± 0.25 mg kg^{-1} and 0.18 ± 0.04 mg kg^{-1}, respectively. After the closure of the BCS, total C and total N values were 1.59 ± 0.25 mg kg^{-1} and 0.20 ± 0.04 mg kg^{-1} respectively. The 0-5 cm sediment interval had a significant increase in concentration of both the Total C and N (student t-test). It the 5-10 cm segment intervals, the BCS preopening concentration for TC and TN were 1.43 ± 0.5 mg kg^{-1} and 0.15 ± 0.04 mg kg^{-1}, respectively. After the closure, the TC and TN concentrations were significantly lower at 1.41 ± 0.28 mg kg^{-1} and 0.16 ± 0.04 mg kg^{-1} in the 5-10 cm segment intervals.

2.4.2 Phosphorus Fractionations

The P extracted with KCl represents the most bioavailable P pool that is loosely bound to sediment particles for algae uptake and present in the porewater. Before the spillway opening, the KCl P pool averaged 0.90 ±0.19 mg kg^{-1} and 1.56 ± 0.27 mg kg^{-1} P for the 0-5 cm and 5-10 cm segment intervals, respectively. This pool accounted for only 0.16 % and 0.29 % of the total P pool in the sediment (Table 2). After the closure of the BCS, the KCl pool was significantly higher at 1.10 ± 0.04 mg kg^{-1} in the 0-5 cm and 1.96 ± 0.16 mg kg^{-1} in the 5-10 cm sediment intervals. This readily available P holds the least amount of P concentration but with a ~ 24 % increase due to the BCS opening; it is an

important factor for nutrient release to potentially stimulate primary production in the water column. This also indicates that majority P is bounded to minerals within the sediment particles.

Table 2.2. Average P concentration (mg kg^{-1}) from 0-5 cm and 5-10 cm segment intervals and the percentage change before and after the 2011 BCS event, standard deviation, and the percent change of each P pool. (* significant level $P < 0.05$ from a Student's T test).

0-5 cm Sediment Intervals			
Phosphorus Pools	Pre-Opening (mg kg^{-1})	Post-Closure (mg kg^{-1})	Change (%)
Readily Available [Pi]	0.90 ± 0.19	1.10 ± 0.04	22 *
Fe/Al bound [Pi]	64.5 ± 8.6	93.2 ± 5.92	44 *
Alkali Organic P [Po]	87.9 ± 11.1	87.7 ± 7.48	0
Ca/Mg bound [Pi]	250 ± 12.2	217 ± 21.4	-13 *
Residue [Po]	145 ± 10.9	289 ± 19.4	100 *
Sum of Total P	547 ± 21.7	689 ± 55.5	26
Total P	525 ± 16.1	677 ± 11.4	29 *

5-10 cm Sediment Intervals			
Phosphorus Pools	Pre-Opening (mg kg^{-1})	Post-Closure (mg kg^{-1})	Change (%)
Readily Available [Pi]	1.56 ± 0.27	1.96 ± 0.16	25 *
Fe/Al bound [Pi]	80.6 ± 18.4	97.3 ± 4.64	21 *
Alkali Organic P [Po]	83.5 ± 8.3	75.6 ± 6.25	-9 *
Ca/Mg bound [Pi]	256 ± 13.2	256 ± 20.5	0
Residue [Po]	126 ± 7.2	235 ± 14.2	87 *
Sum of Total P	547 ± 25.5	666 ± 57	22
Total P	515 ± 19.4	656 ± 10.9	27 *

The most abundant P fraction was associated with Ca and Mg. In similar, predominately anaerobic lake sediment, the sediments were dominated by the Ca and Mg bound P (Reddy et al., 1998). The P concentration of this pool was 250 ± 12.2 mg kg^{-1} in

0-5 cm sediment interval and 256 ± 13.2 mg kg^{-1} in the 5-10 cm before the opening; which accounts for ~ 46 % of the total P pool. The P concentration after the BCS closure was 217 ± 21.4 and 256 ± 20.5 mg kg^{-1} in the 0-5 cm and 5-10 cm segment intervals, respectively (Table 2.2). The Ca and Mg bound pool decrease by 13 % in the 0-5 cm sediment interval and no change in the 5-10 cm segment interval of the total P in the sediment. This is likely due to the lower concentration of P bound to this fraction that was incoming from the Mississippi River. These findings are comparable with research that documented a relative decrease in the amount of Mg concentrations after the 1997 BCS operation (Waters et al., 2009).

The Fe and Al bound P extraction yielded an average concentration of 64 ± 8.6 mg kg^{-1} in 0-5 cm sediment interval and 81 ± 18.4 mg kg^{-1} in the 5-10 cm before the opening; and 93 ± 6.0 mg kg^{-1} in 0-5 cm and 97 ± 4.6 mg kg^{-1} in the 5-10 cm sediment intervals after the BCS closure. The opening of the BCS increased the P concentration from the iron and aluminum pool by 44 % in the 0-5 cm and 21 % in the 5-10 cm intervals. Waters et al. (2009) documented the iron concentration increased by almost 20 % after the 1997 BCS opening event. This result suggests that suspended sediment from the Mississippi River contains higher Fe and Al pools of P.

The sediment alkali organic P concentrations were 88 ± 11 mg kg^{-1} and 83 ± 8 mg kg^{-1} in the 0-5 cm and 5-10 cm intervals respectively, before the BCS opening. After the closure, the P concentrations were 88 ± 7.5 mg kg^{-1} in the 0-5 cm sediment intervals and 76 ± 6.3 mg kg^{-1} in 5-10 cm. The extractable organic fraction remained steady in the 0-5 cm intervals while the 5-10 cm experience on average a 10 % decrease in P

concentration. The calculated residual P concentration was 145 ± 11 mg kg^{-1} and 126 ± 7.2 mg kg^{-1} in the 0-5 cm and 5-10 cm segment interval before the opening, respectively. After the opening, the P concentration was 289 ± 19 mg kg^{-1} for 0-5 cm sediment interval and 235 ± 14 mg kg^{-1} in the 5-10 cm segment interval. The residual P_o, comprised of ~ 25 % of the total P pool before and ~ 38 % after the BCS close. This fraction significantly increased by 89 % in 0-5 cm and 100 % in 5-10 cm segment interval, respectively (Fig. 2.6).

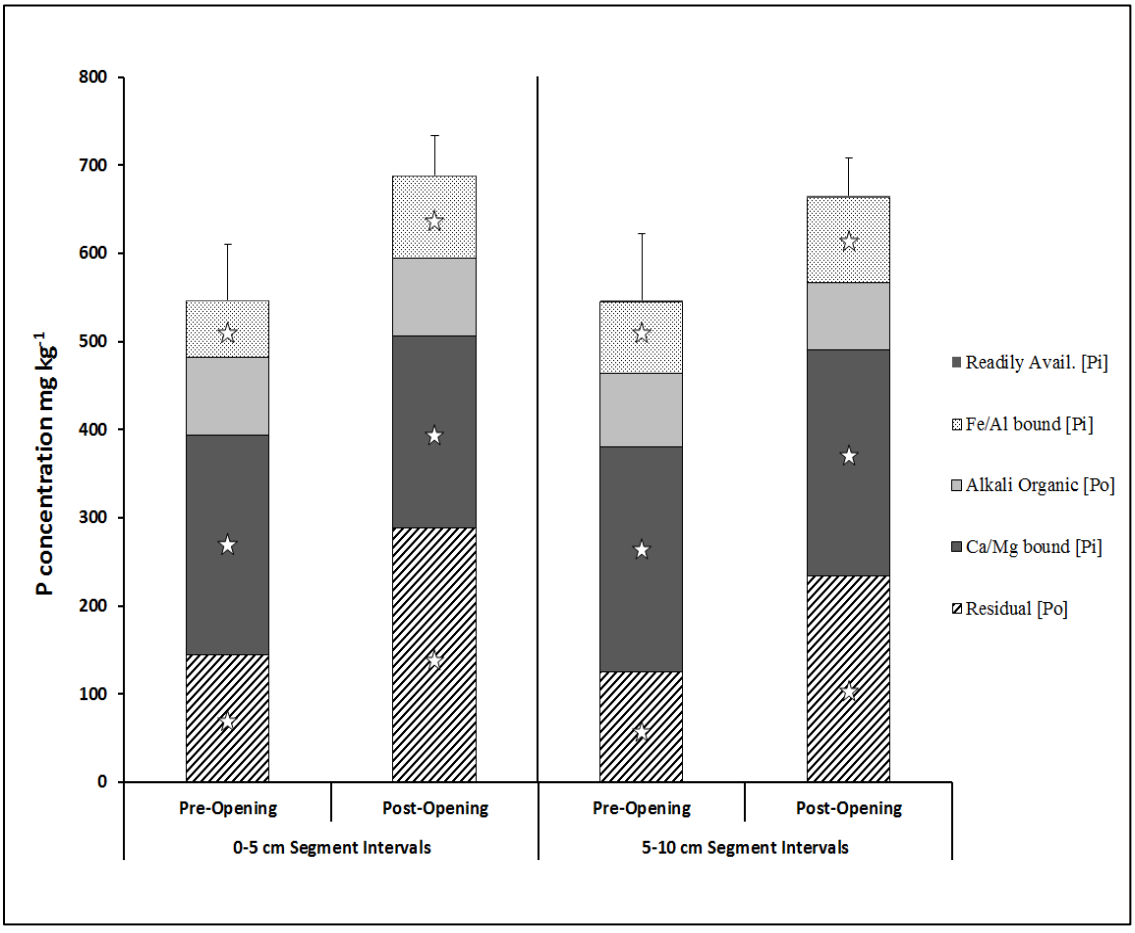

Figure 2.6. Mean P concentration (mg kg^{-1}) of various P fractionations of 0-5 cm and 5-10 cm sediment intervals before and after the closure of the BCS and standard deviation of the total P pools. Student's t test $P < 0.05$ denotes significant differences between P concentrations before and after the 2011 BCS closure is shown with the star symbol.

This residual P consists of complex organic compounds that are resistant to the extraction scheme, and is considered unavailable to organisms in the water column in the short term. These residual P pool can convert into the bioavailable and moderately available forms that can become accessible over longer periods. The residual P pool was a large component of total P suggesting that much of the P in upper sediment layer of the LPE could be released over longer periods of time. In typical estuary sediment, the percentage of residual/unavailable P concentration is lower when compared to wetland systems. This can trigger algal blooms to proliferate in a long term scale (Reddy et al. 2007).

Fabre et al. (2013) calculated that 2.45 Mt of sediment was deposited into the LPE during the Bonnet Carré Spillway opening in 2011. We can use the summation of the various fractions from the P fractionation scheme with the total P of the lake sediments to assess the accuracy of the fractionation method. The average TP summation before the opening is ~ 547 mg kg^{-1} for sediment intervals from 0-5 cm and ~ 547 mg kg^{-1} for sediment intervals from 5-10 cm sediment interval. While the post closure TP concentration was ~ 689 mg kg^{-1} and ~ 667 mg kg^{-1} from 0-5 cm and 5-10 cm sediment intervals, respectively. When comparing the average summation of TP to the measured TP concentration, the accuracy of the fractionation method was found to be 105 % before the opening and 102 % after the closure of the BCS from the 0-10 cm sediment intervals.

2.5 Conclusion

Total P analysis revealed a significant increase of total P in the 0-10 cm sediment interval as a result of the 2011 BCS opening. A sequential P fractionation found that

there were also significant increases in the readily available P, Fe/Al bound P, and residual P fractions. The alkali organic P fraction had no change, while the Ca/Mg bound P decreased. The majority of the total P is potentially available for eventually release to the water column and could potentially trigger algal blooms. High accumulation of P from these diversion opening events created a mechanism for internal P loading in LPE that could potentially aid in triggering seasonal algal blooms. Historically, the LPE already experienced elevated concentrations of P in the sediment but the BCS event increased the TP load in the system.

In the future, climate change may have a role in increasing P load as a result of increased frequency of flooding, which would requires more frequent operation of the spillway. This increase will lead to greater accumulation of P in the sediment that will alter the P cycling of the LPE. If the rate of accumulation of P in the sediment continues to increase, then future lake-wide monitoring and reductions of the amount of external P loading from the northern tributaries will have to be implemented to balance out the increase P inputs from the Mississippi River.

There are no comprehensive studies on the various P pool fractionation concentrations on the sediment, and this fractionation process is the first to be done on the LPE. With these data, more information about the physical and chemical aspects of the system can be monitored to maintain a healthy water quality in the LPE. Lake algal blooms experienced in 1997 and 2008 can be predicted and managed with information about the P internal flux from the lake sediment. In the future, calculations of each P pools percentage can be determined by measuring the total P incoming from the BCS after each opening. From this study, it has been shown that sediments should be

monitored after spillway opening events to determine increases in sediment P. Future work should focus on the amount of time required for the additional P to flux out of the sediment coupled with close monitoring of associated algal blooms.

CHAPTER THREE: POTENTIAL PHOSPHORUS LEGACY OF THE 2011 BONNET CARRÉ SPILLWAY OPENING ON LAKE PONTCHARTRAIN PHOSPHORUS CYCLING

3.1 Introduction

Human construction of dams and diversions along large rivers can be traced back to as early as 2,600 BC in ancient Egypt (Bazza, 2007). Near the beginning of the 21st century, an estimated 77 % of the total volume of water discharged in the upper northern hemisphere has been altered due to human engineering that affects the hydrological features of rivers (Dynesius and Nilsson, 1994). Altering riverine hydrology using diversions, dams, and levees protects cities and farms, but can also influence the functions of adjacent wetlands, organisms dependent on these habitats, and nutrient cycling (Dynesius and Nilsson, 1994). One example of large-scale hydrologic manipulation is the levee modifications to control the Mississippi River basin, which started in the early 1900's (Clay, 1986).

In coastal Louisiana, there are plans to use large-scale Mississippi River diversions to transport freshwater and suspended sediment to deltaic wetlands for restoration purposes (Louisiana Coastal Master Plan, 2012). Controlled river diversions are an effective method to spread sediment-carrying floodwater and to restore the sediment-starved wetlands in Louisiana (Allison and Meselhe, 2010; DeLaune et al., 2003). Large river diversions in the scale of the Bonnet Carré Spillway are expected to best mitigate wetland loss by periodically discharging large pulses of sediment to areas that currently are sediment starved (Wang et al., 2014). These large-scale diversions are

vital to mitigating coastal land loss that is influenced by both sea level rise and ongoing land subsidence.

The BCS was not built to divert sediment; rather its purpose is to divert the Mississippi River's surface water during high flow events into the LPE to protect low lying cities such as New Orleans. In the summer of 2011, the BCS was opened by the U.S. Army Corps of Engineers, for the 10th time in its 80-year history, to reduce high flood water levels and pressure on the river's levee systems (USACE, 2011). The water in the MSR below the Old River Control Structure peaked at 45,704 m^3 million cubic feet in 2011. This was the highest river water discharge ever recorded at this station since it began recording more than 75 years ago. The BCS was opened from May 9 to June 19, with a discharge up to 8,920 $m^3 s^{-1}$, 26 % above flood control design (Allison et al., 2013).

The BCS discharge of large volumes of nutrient-rich water can influence the biogeochemistry in the receiving basins. Increasing levels of nutrient concentrations in the MSR have been driven by the increased use of fertilizer in agriculture within the Mississippi River Basin (Anderson et al., 2008). After the April 2008 opening of the BCS, evidence of harmful algal blooms (HABs) blue-green algae was present in the LPE (Mize and Demcheck, 2009). These harmful blooms occur when conditions of warm temperatures, calm weather, low turbidity water, and elevated nutrient input occur in the water column. Although algal mats covered majority of the lake's water surface, it only extended a few inches into the water column (Bargu et al., 2011). One common cyanobacteria species of blue-green algae was seen in the LPE following the 2008 BCS

opening. These N-fixing species are capable of producing neurotoxins that may cause skin irritations and damaging liver functions in humans and have a deadly effect on aquatic organisms. The proliferation of large algal blooms due to enriched nutrients in the water column leads to eutrophication (Carpenter et al., 1998). Microbacterial decomposition of algae reduces the dissolve oxygen levels in the water column. When the water column is at < 2.0 mg/L, the condition is defined as hypoxia.

The LPE is normally an N-limited system but can change into a P-limited system due to immense loads of inorganic nitrogen delivered during BCS events (Roy et al. 2013). In a eutrophic lake system, much of the dissolved inorganic P (DIP) is rapidly assimilated due to biological uptake in the water column (Reddy et al., 1993). The last three recent BCS openings in response to flood events have loaded: 15,299 Mt of dissolved inorganic N (DIN) and 584 Mt of DIP in 1997; 9,938 Mt of DIN and 375 Mt of DIP in 2008; and 26, 085 Mt of DIN and 1,122 Mt of DIP in 2011 (Roy et al., 2013). Eutrophication is a major concern when excessive amounts of bioavailable P and N enter an estuarine system (Nixon, 1995). Monitoring of past BCS openings show that cyanobacteria blooms can occur in the summertime after the closure of the BCS, dependent on many interrelated factors (Roy et al., 2013). When DIN is available in abundance, the uptake of PO_4^+ by primary producers can deplete the DIP resource in the water column. This paucity of P in turn enhances the flux of DIP from estuarine sediments, which can contribute to subsequent blooms of phytoplankton (Roy et al. 2012). In an ecosystem like the LPE, the DIN:DIP molar ratio is extremely important to the phytoplankton dynamics of the system. With the changing global climate and warmer temperature that could potentially increase large amounts of snow melts from the

northern U.S. More occurrences of these large scale river diversions will continue to load excess amount of nutrients. This could lead to an increased frequency of HABs. Understanding the role of these internal P pools and the methods of P fluxing from these pools in the LPE can help reduce toxic HABs in the system.

3.2 Accumulation of P in the Sediment

Bonnet Carré Spillway openings allow nutrient rich sediment floodwater to enter the LPE. Over time, the suspended sediment, which contains substantial amount of P, settles onto the Lake bed surface. This accumulation of P rich sediment may serve as a long-term source of P to the LPE water column. In sediments, physicochemical and biological processes interact to regulate the amount of P that is released to the water column. Short term P storage can occur in microbial biomass in the sediment (Reddy et al., 2011). Phosphorus can be bound to variety of inorganic sediment components, depending on the sediment characteristics and biogeochemical processes (Stumm and Leckie, 1971). Phosphorus is deposited in organic and inorganic forms and the ratio of P bound to each depends on the locations and sediment properties. Biogeochemical cycling, concentration of P in the water column, concentration of P in the sediment, total P content, and biological activities all affect the DIP concentration gradient at the sediment-water interface in an estuarine system.

The LPE sediments can act as both sink and source of inorganic P to the water column. Biotic and abiotic factors greatly increase the rate or net movement of P in the sediment and across the sediment-water interface. Biotic components are living organisms that have an effect on P cycling in the ecosystem. These components can

include: micro-organisms in the sediment, macrophytes, and plankton. Abiotic, physical processes that can affect P cycling in the estuary include: sedimentation, physical mixing in the water column, sediment suspension and redox conditions. Soluble P can migrate vertically from the surface sediment up to the water column in response to the concentration gradient in DIP (i.e., higher in the sediment porewater, lower in the water column).

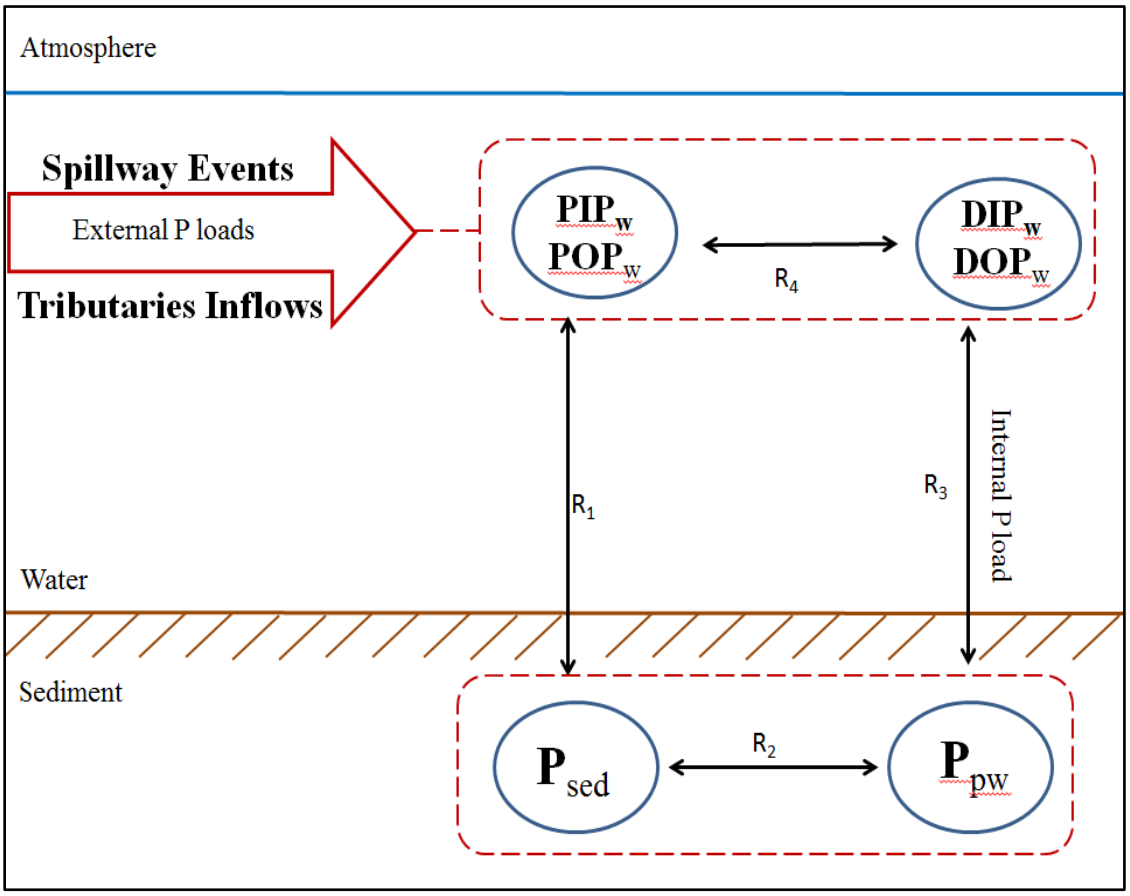

Figure 3.1. Diagram of various forms of P, pools and transformation pathways of P in the Lake Pontchartrain estuary. Rates (R) are defined in the main text.

A major source of P entering in the LPE system during seasonal flooding comes from tributaries inflows from the northern portion of the Lake, diversions, and spillway

openings (Fig. 3.1). Incoming external P loads can enter the system as dissolved and particulate organic and inorganic P. Particulate P includes that bound to sediment particles. Over time, the rate movement (R_1) of P descends down into the pore water and eventually accumulates in the sediment layer (Fig. 3.1). The release of P (R_2 and R_3) from the sediment into the water column and vice versa is due to the P equilibrium concentration (EPC_w) in the sediment's pore water and the water column. Uptake of dissolved organic and inorganic P by microorganisms and aquatic plants in the also increase the P rate to flux out into the system. As algae and microorganism die, P is reintroduced back into the sediment, aiding a continuous cycle of P.

Accumulation of sediment-bound P suggests that net total P flux is downward into the sediment and the DIP flux is upward to the water column (Moore *et al.* 1998, Fisher *et al.* 2005). Concentrations of DIP and conditions in the water column influence the DIP diffusive flux rate. Physical events like winds, storms, and tides also impact the DIP flux rate by resuspending sediments. Resuspension of sediments results in high turbidity levels and can increase the total P concentration of the water column. Songeraad (1992) found that resuspension of sediments caused by wind on a shallow lake increased the internal P loading rate by 20 to 30 times, comparing with an undisturbed sediment layer.

Quantification of the internal P load is a critical step to improving water quality conditions, particularly in shallow eutrophic estuary. Even when sediments are implicated as a major source of nutrients, reductions in external P load must be included in any management plan to alleviate eutrophication, since external inputs of P ultimately accumulate in the sediments and cause future internal loading. A constant anoxic condition creates an optimal situation for the release of P, which may not naturally occur

in the Lake. Thus, anoxic treatments may overestimate sediment P release; therefore, it may be best to think of release rates measured in anoxic treatments as maximum potential rates.

In order to calculate annual internal P load, assumptions about the timing, duration, and spatial extent of hypolimnetic anoxia must be made. For example, in strongly stratified systems with relatively consistent water depth and confirmed hypolimnetic anoxia, some studies have assumed that the entire lake area is anoxic during stratified periods for the purpose of annual internal P load estimation. However, this may result in an overestimation of load due to oxic sediments in shallow littoral areas. Thus, a comprehensive dissolved oxygen monitoring strategy that captures diurnal, seasonal, and spatial variability in redox condition is highly recommended for accurate annual internal load estimation. Under normal condition, the LPE is in aerobic condition in the spring, summer, and during BCS opening events (McCorquodale et al., 2002).

In this study, the major tasks are to (1) compare the P concentration with respect to the distances from the BCS opening, (2) use previous discussed P fractionation data to determine the quantities of P bound in each fraction for the entire surface layer of the LPE, and (3) estimate the amount of time it takes for the newly added P from the BCS event to flux to the water column for the lake to return to pre-opening physical conditions.

3.3 Methods

The movement of P in a system can be calculated using Fick's Law of Diffusion (Eq. 3.1). Where J is the diffusive flow rate per unit area per unit time, D is diffusion

coefficient that is dependent on temperature, fluid's viscosity, and particle size. $\partial\phi$ is the concentration of P per unit volume and ∂x is diffusive distance. The diffusive flux of P concentration is driven from regions of higher concentration to regions of lower concentration, with a magnitude that is proportional to the concentration gradient. Phosphorus flux in sediment is determined by the concentration gradient between dissolved P in the pore water and dissolved P in the water column. In addition to a tortuosity factor related to grain size.

Equation 3.1. $$J = -D \frac{\partial \phi}{\partial x}$$

In order to calculate the P loading rate in the LPE, the TP in the 0-10 cm sediment segment interval is analyzed using (Eq. 3.2). Where TP mass is in kg, TP is in mg kg^{-1} P, Bulk density is g cm^{-3}, and the volume of the sediment from the 0-10 cm layer.

Equation 3.2.

$$\text{TPmass} = (\text{TP}) \text{ x } (\text{Bulk Density}) \text{ x } (\text{ Volume of Lake Sediment})$$

A sequential P fractionation extraction was necessary to calculate the reactive and nonreactive P in the sediment (see Chapter 2). The fractionation scheme included five sequential extractions that determine the readily available P, alkali extractable organic P, iron/aluminum-bound P, calcium/magnesium-bound P, and residual P summing up to the total P in the sediments surface layer. Reactive P consists of P bound to extractions of KCl, NaOH, and HCl. All other extractions are considered unreactive for biological consumption (Reddy et al., 2011). Using the fractionation scheme of sediment core from the 2011 BCS opening event, it was found that 25 % of TP from the 0-10 cm segment

interval are nonreactive P and the remaining 75 % are reactive P before the 2011 BCS operation. After the closure of the BCS, the nonreactive pool was 39 % and the reactive pool was 61 %. These reactive P are able to be released to the water column over a relatively short time scale (years) (Eq. 3.3).

Equation 3.3

$$\text{Years of DIP Flux} = \frac{(\text{TPmass } 0-10 \text{ cm}) \text{ x } (\%\text{ Reactive P})(\alpha)}{(\text{Mean DIP flux rate})}$$

Where the TP_{mass} is Mt, the mean DIP flux rate is Mt yr^{-1}; the % of Reactive P in the sediment 0-10 segment interval, and α indicates the % of reactive P release.

Roy et al. (2012) estimated that under normal anaerobic condition in the sediment, the maximum DIP flux rate was ~ 517 Mt y^{-1}, with the assumption that the muddy particle inhibiting oxygen from diffusing through sediment layer throughout the year. This flux rate was measured before the 2011 BCS opening event. Due to the bioavailability nature of different P forms, the release of P bounded to different fractions in the sediment particle can have an exponentially declining flux rate through time. A study of P in Lake Okeechobee flux indicate that the DIP concentration level increase to the equilibrium P concentration in the water (EPC_w) column at the first ~5 months and gradually decrease over time (Reddy et al. 2007). The release of DIP in a system will be determined by the EPC_w level and uptake by biological activities. In a seasonal flood diversion opening, the internal P mass will increase in the sediment due to rivers and tributary inputs. This increase of TP storage in the sediment due to the BCS opening will contribute to internal P loading from sediments.

3.4 Results

3.4.1 Relationship of P concentrations in comparison with distance

Sediments in suspension play an important role in transporting nutrients and contaminants in aquatic systems. The percentage of each P form is dependent on the sediment grain size and the capacity to bind nutrients in the sediment (Kapanen, 2008). During BCS openings, a portion of the Mississippi river flows into the LPE, discharging sand, silt, and clay sediment fractions. The majority of the nonreactive, heavier sand particles are deposited in the BCS structure and near the entrance of the LPE (Nittrouer et al., 2012). Some sand and the lighter silt particles travel into the LPE; while the clay particles travel farther away from the BCS entrance. Lake Pontchartrain Estuary sediment data show that loss on ignition and moisture content increases with distance from the BCS entrance (Appendix A.3 and A.6; Appendix C.3 and C6). Bulk density, however, decreases with this distance (Appendix B.3 and B.6). Before the 2011 BCS opening, there is no spatial trend in sediment of total P in the 5-10 cm surface sediment layer with distance from the BCS. For the 0-5 cm sediment interval, there are uniformed distributions of TP through the LPE except for two sample stations that have fine sandy grain size, before the opening of the BCS. After the BCS closure, sediment TP concentrations increased in both the 0-5 cm and the 5-10 cm sediment intervals near the BCS , with the effect decreasing with distance from the BCS.

Similar trends are seen after the BCS closure at the 0-10 cm sediment interval for the Fe/Al and Ca/Mg bound P fractions (Fig. 3.3 a, b, c, d). For the residual P fraction, the opposite trend can be observed. As the distances increase from the entrance of the

BCS, the P concentration of the residual P increased after the BCS closure (Fig. 3.3 e, f.). This can also be related to the smaller silt and clay fractions that residual P can be bound. These are characterized by lower settling velocities and therefore can be transported further from the BCS. Unlike the typical distinct trends seen after the closure of the BCS, the P concentrations are mostly uniformed with no patterns with looking at the spatial differences. The Fe/Al bound P 0-5 cm sediment interval concentration was very low at the BCS opening entrance before the 2011 BCS operation (Fig. 3.2 a, b). However, the 5-10 cm sediment interval is continually low in P concentration throughout the LPE. The Ca/Mg fraction and the residual P fraction have no trends in relation with the distance before the BCS opening (Fig. 3.2 c, d, e, and f). This could be caused by disturbance due to surface wind, currents, and tide that influence that constant mixing in the sediment layer.

3.4.2 Phosphorus Flux Estimation

Sediment samples were analyzed for TP before the opening and after the closure of the 2011 BCS opening event. From this, the calculated value of 10,368 Mt of TP was present in the 0-10 cm sediment interval before the 2011 flood event. After the closure of the BCS, the TP load increased by 2,925 Mt to 13,293 Mt of TP in the 0-10 cm sediment interval. The sediment TP significantly increased by 28 % as a result of the 42 days Bonnet Carré Spillway opening. The residual P pool significantly increased by 93% indicating that majority of the TP incoming from the Mississippi River is nonreactive P (Table 3.1). The readily available P pool and P bound to Fe and Al significantly increased by 26 % and 32 %, respectively. This is an important finding because these two P pools are the most likely to become bioavailable.

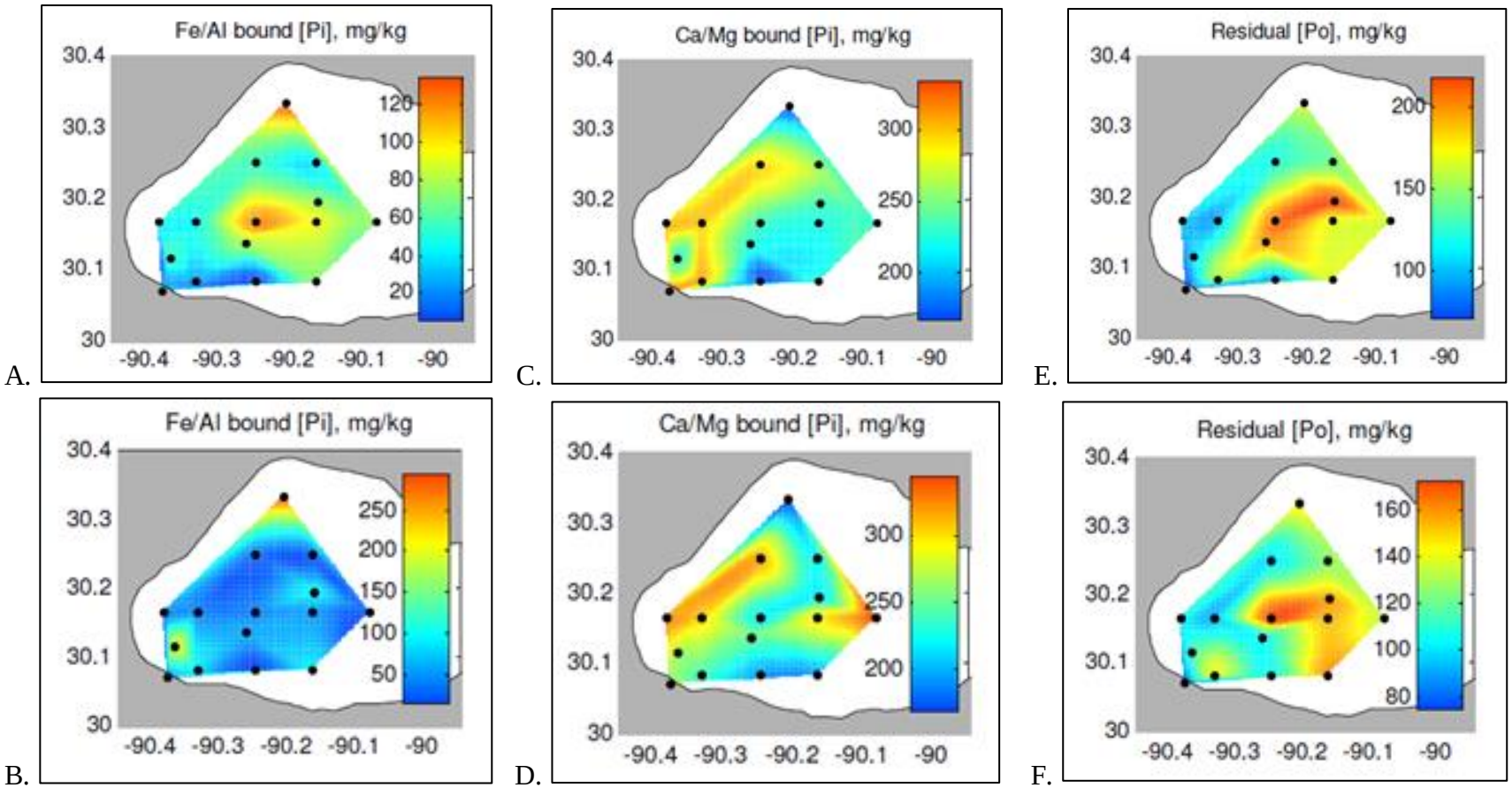

Figure 3.2: Before the 2011 BCS opening P fractions concentrations in correlation from the distance of the BCS mouth of Fe/Al bound P at A) 0-5cm and B) 5-10cm; Ca/Mg bound P at C) 0-5 cm and D) 5-10 cm; and Residual P at E) 0-5 cm and F) 5-10 cm sediment intervals.

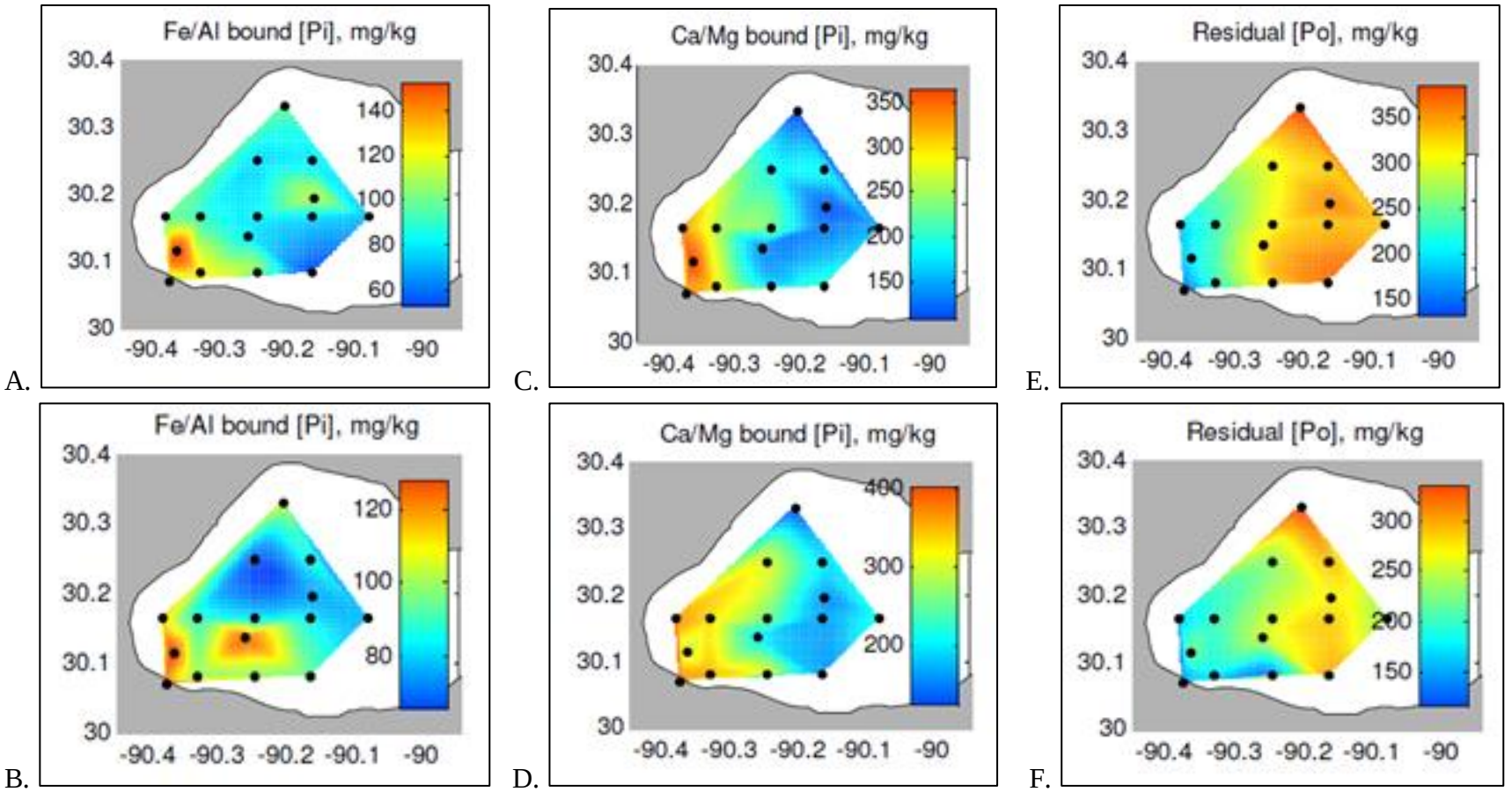

Figure 3.3. 2011 BCS post closure P fractions concentrations in correlation from the distance of the BCS mouth of Fe/Al bound P at A) 0-5cm and B) 5-10cm; Ca/Mg bound P at C) 0-5 cm and D) 5-10 cm; and Residual P at E) 0-5 cm and F) 5-10 cm sediment interval.

These pools of P can most readily flux out of the sediment into the water column under anaerobic sediment conditions and have implications for eutrophication, including summertime algal blooms.

Table 3.1. Various pools of Net P concentration from 0-10 cm segment intervals due to the 2011 Bonnet Carré Spillway event. The percent change of each pool before and after the BCS closure and the amount of time it takes for the new P to flux out from the sediment based on 517 Mt y^{-1} mean flux rate (Roy et al. 2012).

Forms	Net P ($mg\ kg^{-1}$)	Change (%)	Time to Flux Out the Net P (years)
Readily Available [Pi]	67.3	+ 26 *	0.13
Fe/Al Bound [Pi]	410	+ 32 *	0.79
Alkali Organic P [Po]	351	- 4.1	0.68
Ca/Mg Bound [Pi]	994	- 6.5	1.92
Residual [Po]	1141	+ 93 *	2.21
Total	2,925	+ 28	5.66

The alkali organic P and P bound to Ca and Mg exhibited slight decreases (-4% and -7%, respectively), suggesting a negligible source of these P forms from the river sediment (Table 3.1). In this research, it was assumed that the reactive P consist of the readily available P, alkali organic P, Fe/Al bound P, and Ca/Mg bound P. The nonreactive P is the residual P that is tightly bound to the sediment, but which may move into reactive pools and eventually contribute to internal P loading over longer time horizons. Previous research found that the P flux rate from the sediment to the water column is ~517 Mt P y^{-1} (Roy et al., 2012). With an amount of TP before and after the closure of the BCS and a P flux rate, we were able to estimate the time in years it would take for all the P deposited in LPE sediments during the 2011 BCS flood event to flux out of the sediment into the water column.

The concentration of total P and fractions of P are generally higher in recent (newer) sediments that are related to recent P loading (Reddy et al., 2007). As the TP mass increases from the 2011 BCS opening onto the LPE, this will increase the potential for DIP flux from the sediment to the water column. After excessive TP loading onto the sediment layer of the LPE due to the 2011 BCS opening, DIP began to flux up towards the lower concentration water column. Dissolved inorganic P will continue to flux into the water until the LPE reaches the EPC of ~ 0.07 mg DIP-P L^{-1}. This EPC has been observed in both laboratory sediment core incubations (Roy et al., 2012) and in water column field measurements following the 2011 spillway event (Roy et al., 2013).

The net difference of sediment TP mass from the 2011 BCS opening event was 2,925 Mt of P. This accumulation of P may amplify an internal feedback in Lake Pontchartrain and increase the P concentration equilibrium between sediment pore water and the water column in the system. By using the same DIP flux rate, it is estimated that it would take ~ 6 years for all the newly TP, which includes the reactive and non-reactive pool, added into from the 2011 BCS diversion opening event for the LPE to get back to its preopening P level baseline. It would take ~ 0.9 years to flux out 25 % of reactive P, ~ 1.8 years to flux out 50 % of reactive P, and ~ 3.5 years to flux out 100 % of reactive P in the surface layer of the LPE (Fig. 3.4). When under acidic conditions, caused by microbial activities or increase of CO_2 in the water column, the nonreactive pool fraction will dissolve and become more available in the reactive pool in the water column. It is therefore possible for 100 % of the newly added P in the nonreactive pool to move into reactive pools over time and eventually diffuse into the LPE water column.

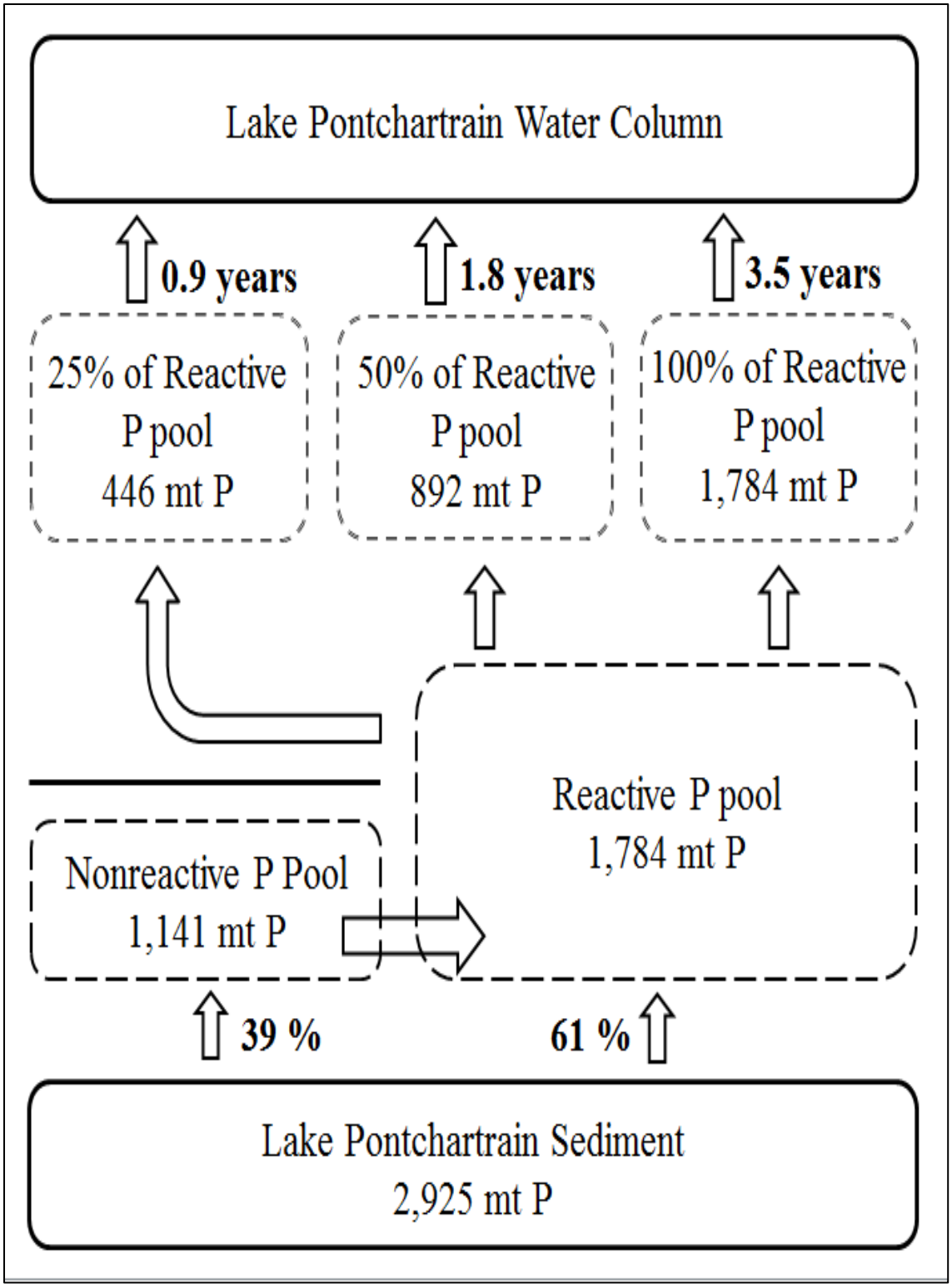

Figure 3.4. Time duration of potential internal phosphorus loading from Lake Pontchartrain sediments based on different assumptions (α) before the 2011 Bonnet Carré Spillway Event.

Internal organic P pool from decomposing phytoplankton pools and other biological activities can aid in this process. There are many factors that determine the time scale for the reactive and nonreactive P pools to flux out from the sediment pore water to the lake water column. Further studies of P flux rate for the LPE need to be performed to fully understand the P movement, but a range of 50 % to 100 % of reactive P flux out from the sediment is very probable to occur.

The DIP flux calculation that we used is based on a linear rate provides a reasonable first estimate. However, internal P loading is unlikely to always occur in a linear fashion. For example, Reddy et al. (2007) show that P flux is nonlinear depending of the concentration of the equilibrium P concentration in the water column and the TP concentration in the sediment pore water. Nitrogen limitation in the LPE could limit DIP assimilation by phytoplankton at times, which has the indirect effect of allowing water column DIP to reach EPC, thereby minimizing the DIP concentration gradient between the sediment pore water and the water column, limiting DIP flux (Roy et al. 2013). Seasonal effects such as temperature changes, winds, and hurricanes could also occur.

My estimate here of 6 years (Fig. 3.5, Linear model P Flux) for all newly deposited P from the BCS to flux from the sediments to the water column could be either an underestimation or an overestimation. Previous nonlinear models of diffusive flux (Reddy et al., 2007) suggest that the rate of diffusion of P from the sediments to the water column can slow over time, thereby increasing the number of years it would take for all of the P to flux out. Alternatively, advective flux caused by resuspension of sediments by wind-waves could cause the P deposited during the BCS opening to move into the water

column much faster than I have estimated here using a flux rate that only accounts for diffusion (Roy et al. 2012).

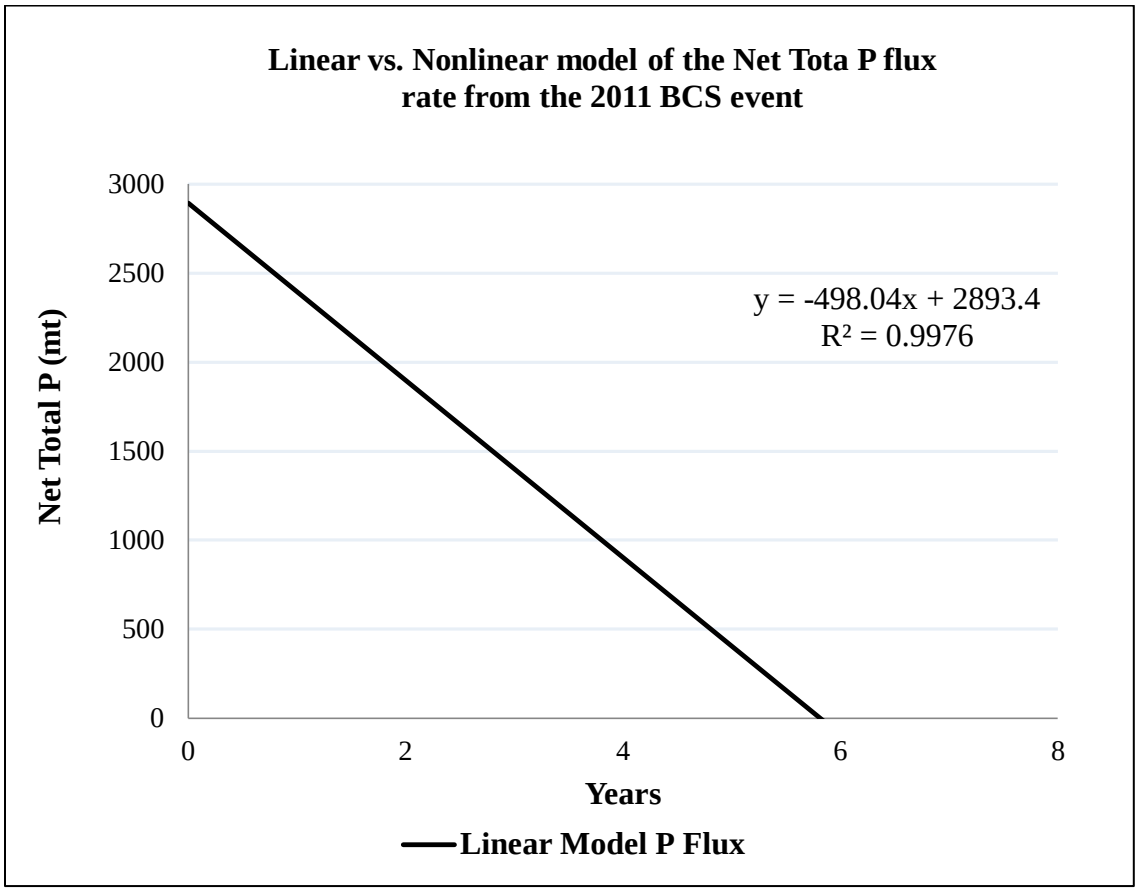

Figure 3.5. Linear flux rate estimate of the newly added TP from the 0-10 cm sediment interval after the closure of the 2011 Bonnet Carré Spillway.

3.5 Conclusion

The estimated total P mass in Lake Pontchartrain 0-10 cm sediment interval before the opening of the Bonnet Carré Spillway was 10,368 Mt P. The total P increased by 28 % to 13,293 Mt P after the 42-day BCS event. A time of 6 years can be estimated for all of the newly added sediment TP to flux out from the sediment and into the water column using a linear flux model determined from a laboratory core incubation. This

estimation is the amount of time is needed for the P in the LPE sediment to recover back to the pre-opening baseline assuming diffusive flux. However, the sediment resuspension from winds could, in short bursts of time, increase the flux rate of P into the water column. It is t important to understand the legacy impact of diversions on P biogeochemistry in the receiving basin as opening can happen in closely spaced succession (2008 and 2011, for example). Increasing the internal P load in the LPE system can potentially support increased bloom frequency of harmful cyanobacteria, especially N-fixers. With an estimation of ~ 6 years to flux out majority of the added TP in the sediment surface layer, and the rate of the BCS opening more frequently (average of 4.7 years for the last 3 BCS opening events), it is possible that another BCS opening may occur before added P from the 2011 event has fluxed out. The ability in limiting Mississippi River discharges into the LPE is highly restricted because protecting urban areas from flooding is a priority. Therefore, management of P sources within local watersheds is one option to address excessive P introduction to the LPE (Roy et al., 2014). The internal P loading and the EPC in the water column will continue to increase as each BCS opening occur in the future if they are closely spaced. Each future BCS or any diversion opening will have an effect on the legacy of P in the sediment long after the operation is done. While the immediate water quality implications of BCS openings have been discussed in the literature and media, we must also consider that the effects of diversions on estuarine biogeochemistry which may last for many years.

CHAPTER FOUR: CONCLUSIONS

Internal P loading in the LPE is an important issue that affects the water quality and organisms that inhabit this system. A sequential P fractionation was performed before and after the 2011 Bonnet Carré Spillway opening to examine the impact of these large river diversion operations on estuarine P biogeochemistry. Before the opening of the 2011 BCS, 10,368 Mt of P were found in the 0-10 sediment interval. After the closure of the BCS, 13,293 Mt of P were found in the 0-10 sediment interval, an increase of 28 % due to the 42 days BCS opening. The residual P showed the greatest increase at ~ 93 %. While the Ca/Mg bound P decreased and the alkali organic P exhibited no significant change in the TP. The Fe/Al bound P and the most readily available P increased by 32 % and 26 %, respectively. Majority of the fine sand fraction can be found near the BCS entrance and the grain size gradually decreases in size as the lighter, muddy particle traveled farther away from the BCS entrance. The Fe/Al and the Ca/Mg bound P concentration decreased as the distance from the BCS increase, while the reverse trends can be seen for the residual P. A 2,925 net accumulation of P mass was deposited during the whole 2011 BCS operation. Using the flux rate from a previous laboratory core flux study (Roy et al., 2012), an estimated time of ~ 6 years are necessary to flux out all the newly added TP by diffusive flux. Depending on the number of BCS openings over a certain time span, the P baseline could steadily increase or remain at baseline. If the rate of BCS opening is greater than the time it takes for net TP to flux back out of the water column, there will be an increase in accumulation of TP in the LPE system. An increase in TP in the sediment due to these diversion openings will affect the LPE water quality into the future potentially impacting the estuarine ecology.

LITERATURE CITED

Allison, M.A., and Meselhe, E.A., (2010). The use of large water and sediment diversions in the lower Mississippi River (Louisiana) for coastal restoration. Journal of Hydrology 387: 346-360.

Allison, M.A., Vosburg, B.M., Ramirez, M.T., and Meselhe, E.A., (2013). Mississippi River channel response to the Bonnet Carré Spillway opening in the 2011 flood and its implications for the design and operation of river diversions. Journal of Hydrology 477: 104-118.

Anderson, D.M., Burkholder, J.M., Cochlan, W.P., Glibert, P.M., Gobler, C.J., Heil, C.A., Kudela, R.M., Parsons, M.L., Jack Rensei, J.E., Townsend, D.W., Trainer, V.L., and Vargo, G.A., (2008). Harmful algal blooms and eutrophication: Examining linkages from selected coastal regions of the United States. Harmful Algae 8: 39-53.

Anderson, J.M., (1976). An ignition method for determination of total phosphorus in lake sediments. Water Research 10: 329-331.

Austin, J., (1999). U.S. Army Corps of Engineers, New Orleans District, oral presentation.

Bargu, S., White, J.R., Li, C., Czubakowski, J., and Fulweiler, W., (2011). The progressive changes on nutrients, phytoplankton biomass and toxin production in an oligohaline estuarine lake after a short term river water pulse. Hydrobiologia 66: 377-389.

Bazza, M. (2007). Overview of the history of water resources and irrigation management in the Near East**.** Water Science & Technology 7: 201-209. DOI:10.2166/ws.2007.023.

Carpenter, S.R., Caraco N.F., Correll D.L., Howarth R.W., Sharpley A.N., and Smith, V.H., (1998). Nonpoint pollution of surface waters with phosphorus and nitrogen. Ecological Applications 8: 559-568.

Chao, X., Jia, Y., and Hossain, A., (2010). Numerical Modeling of Flow and Sediment Transporting Lake Pontchartrain due to Flood Release from Bonnet Carré Spillway. Sediment Transport Processes and Their Modelling Applications. Andrew J. Manning (Ed.). ISBN 978-953-51-1039-2, InTech, 14:357-380, DOI: 10.5772/54435.

Clay, F.M., (1986). A Century on the Mississippi: A History of the Memphis District U.S. Army Corps of Engineers 1876-1981. U.S. Army Corps of Engineers Memphis District, Memphis, Tennessee pp. 293.

Codron, L., and Newman, S., (2010). Revisiting the fundamental of phosphorus fractionation of sediments and soils. Journal of Soil Sediments 11:830-840. DOI 10.1007/s11368-011-0363-2

Crocker, J.A., (1988). Sediment deposition in Lake Pontchartrain from the 1973 Bonnet Carré Spillway operation: New Orleans, LA, University of New Orleans, Department of Geology and Geophysics, M.Sc. thesis, p.81.

DeLaune, R.D., Jugsujinda, A., Peterson, G.W., and Patrick Jr., W.H., (2003). Impact of Mississippi River freshwater reintroduction on enhancing marsh accretionary processes in a Louisiana estuary. Estuarine Coastal Shelf Science 58: 653-662.

Dortch, Q., Peterson, J., and Turner, R., (1998). Algal bloom resulting from the opening of the Bonnet Carré spillway in 1997. Fourth Bi-annual Basics of the Basin Symposium. United States Geological Survey: 28-29.

Dynesius, M., and Nilsso, C., (1994). Fragmentation and Flow Regulation of River Systems in the Northern Third of the World. Science 266: 753-762.

Fabre, J.B., (2012). Sediment flux and fate for a large-scale diversion: the 2011 Mississippi River flood, the Bonnet Carré Spillway, and the implications for coastal restoration in south Louisiana. Louisiana State University.

Flocks, J., Kindinger, J., Marot, M., and Holmes, C., (2009). Sediment Characterization and Dynamics in Lake Pontchartrain, Louisiana. Journal of Coastal Research 54:113-126.

Frossard, F., Brossard M., Hedley, M.J., and Metherell, A., (1995). Reactions controlling the cycling of P in soils. In H. Tiessen (ed.) Phosphorus in the global environment: Transfers, cycles and management. John Wiley & Sons, NY, p. 107-137.

Haggard, B.E., and Sharpley, A.N., (2007). Phosphorus transport in stream: Processes and modeling considerations. In D. Radcliffe and M. Cabrera (eds.), Modeling phosphorus in the environment. CRC Press, Boca Raton, FL. p. 105-130.

Jensen, H.S. and Anderson, F.O., (1992). Importance of temperature, nitrate, and pH for phosphate release from aerobic sediments of four shallow, eutrophic lakes. Limnology and Oceanography 37: 577-589.

Li, C.Y., Walker, N., Hou, A.X., Georgiou, I., Roberts, H., Laws, E., McCorquodale, J.A., Weeks, E., Lie, X.F., and Crochet, J., (2008). Circular plumes in Lake Pontchartrain estuary under wind straining. Estuarine, Coastal and Shelf Science 80:161-172.

Malecki, L., White, J., and Reddy, K., (2003). Nitrogen and Phosphorus Flux Rate from sediments in the Lower St. Johns River Estuary. Journal of Environmental Quality 33: 1545-1555.

Malecki-Brown, L.M., and White, J.R. (2009). Phosphorus sequestration in aluminum amended soils from a municipal wastewater treatment wetland. Soil Science Society of American Journal 73: 852-861.

Manheim, F.T., and Hayes, L., (2002). Sediment database and geochemical assessment of Lake Pontchartrain Basin. Lake Pontchartrain Basin: Bottom Sediments and Related Environmental Resources: U.S. Geological Survey Professional Paper 1634.

McCorquodale, J.A., Roblin, R.J., Georgiou, I.Y., and Haralampides, K.A., (2009). Salinity, nutrient, and sediment dynamics in the Pontchartrain Estuary. Journal of Coastal Research 54: 71-87.

McCulloch, J., Gudimov, A., Arhonditsis, G., Chesnyuk, A., and Dittrich, M., (2013). Dynamics of P-binding forms in sediments of a mesotrophic hard-water lake: Insights from non-steady reactive-transport modeling, sensitivity and identifiability analysis. Chemical Geology 354: 216-232.

Mize, S.V., and Demcheck, D.K., (2009). Water quality, phytoplankton communities in Lake Pontchartrain during, after the Bonnet Carré Spillway opening, April to October 2008 in Louisiana, USA. Geo-Marine Letters 29: 431-440.

Moore, P.A., and Reddy, K.R., (1994). Role of Eh and pH on phosphorus geochemistry in sediments of Lake Okeechobee, Florida. Journal of Environmental Quality 23: 955-964.

Nittrouer, J., Best J., Brantley, C., Cash, R., Czapiga, M., Kumar, P., and Parker, G., (2012). Mitigating land loss in coastal Louisiana by controlled diversion of Mississippi River sand. Nature Geoscience 5:534-537. DOI: 10.1038/NGEO1525.

Ogdahl, M. E., Steinman, A. D., and Weinert, M. E., (2014). Laboratory-determined Phosphorus Flux from Lake Sediments as a Measure of Internal Phosphorus Loading. Journal of Visual Experiment 85: e51617. DOI:10.3791/51617.

Pant, H.K., and K.R. Reddy. (2001). Phosphorus sorption characteristics of estuarine sediments under different redox conditions. Journal of Environmental Quality 30:1474-1480.

Patrick, W.H., Williams B.G., and Morghan, J.T., (1973). A simple system for controlling redox potential and pH in soil suspensions. Soil Science Society of America Proceeding 37: 331-332.

Peters, R.H., (1986). The role of prediction in limnology. Linmology Oceanography: 31 1143-1159.

Reddy, K.R., and DeLaune, R.D., (2008). Biogeochemistry of Wetlands: Science and Application. CRC Press Boca Raton Taylor and Francis Group.

Reddy, K.R., DeLaune, R.D., DeBusk, W.F., and Koch, M., (1993). Long-term nutrient accumulation rates in the Everglades wetlands. Soil Science Society of America Journal 57: 1145-1155.

Reddy, K.R., Fisher, M.M., Wang, Y., White, J.R., and James, T.A., (2007). Potential effects of sediment dredging on internal phosphorus loading in a shallow, subtropical lake. Lake and Reservoir Management 23: 27-38.

Reddy, K.R., Newman, S., Grunwald, S., Osborne, T.Z., Corstanje, R., Bruland, G., and Rivero, R., (2005). Spatial distribution of soil nutrients in the Greater Everglades Ecosystem. Final Report. South Florida Water Management District, West Palm Beach, FL.

Reddy, K.R., Newman, S., Osborne, T.Z., White, J.R., and Fitz, H.C., (2011). Phosphorus Cycling in the Greater Everglades Ecosystem: Legacy Phosphorous Implications for Management and Restoration. Environmental Science and Technology 41:149-186.

Reddy, K.R., Wang, Y., DeBusk, W.F., Fisher, M.M., and Newman S., (1998). Forms of sediment phosphorus in selected hydrologic units of the Florida Everglades. Sediment Science Society of American Journal 62: 1134-1147.

Reynolds, C.S., and Davis, P.S., (2001). Sources and bioavailability of phosphorus fractions in freshwater: a British perspective. Biological Review 76: 27-64.

Roy, E.D., White, J.R., Seibert, M., (2014). Societal Phosphorus metabolism in future coastal environments: insights from recent trends in Louisiana, USA. Global Environmental Change 28:1-13.

Roy, E.D., Nguyen, N.T., Bargu, S., and White, J.R., (2012). Internal loading of phosphorus from sediments of Lake Pontchartrain (Louisiana, USA) with implications for eutrophication. Hydrobiologia 684: 69-82.

Roy, E.D., White, J.R., Smith, E.A., Bargu, S., and Li, C. (2013). Estuarine ecosystem response to three large-scale Mississippi River flood diversion events. Science of the Total Environment 458-460: 374-387.

Sharpley, A.N., Menzel, R.G., Smith, S.J., Rhoades, E.D., and Olness, E.A., (1981). The sorption of soluble phosphorus by soil material during transport in runoff from cropped and grassed watersheds. Journal of Environment Quality 10: 211-215.

Signell, R.P., and List, J.H., (1997). Modeling Waves and Circulation in Lake Pontchartrain. Gulf Coast Association of Geological Societies Transactions 47: 529-532.

Sondergaard, M., Kristensen, P., and Jeppesen, E., (1992). Phosphorus release from resuspended sediment in the shallow and wind exposed Lake Arreso, Denmark. Hydrobiologia 228: 91-99.

State of Louisiana. (2012) Louisiana's Comprehensive master plan for a sustainable coast. http://www.coastalmasterplan.louisiana.gov/2012.

Stumm, W., and Leckie, J.O., (1971). Phosphate exchange with sediments; its role in the productivity of surface waters. Proc. 5. International Water Pollution Research Conference, Pergamon Press, London.

Turner, B.L., Newman, S., and Reddy, K.R., (2006). Overestimation of organic phosphorus in wetlands soils by alkaline extraction and molybdate colorimetry. Environmental Science and Technology 40: 3349-3354.

Turner, R.E., Dortch, Q., Justic, D., and Swenson, E.M., (2002). Nitrogen loading into an urban estuary: Lake Pontchartrain (Louisiana, U.S.A.). Hydrobiologia 487: 137-152.

Turner, R.F., Dortch, Q., Rabalais, N., (1999). Effects of the 1997 Bonnet Carré Opening on Nutrients and Phytoplankton in Lake Pontchartrain. Final report submitted to the Lake Pontchartrain Basin Foundation, pp. 117.

U.S. Environmental Protection Agency, (1993). Methods for the determination of inorganic substances in environmental samples. Environmental Monitoring Systems Laboratory, Cincinnati.

US Army Corps of Engineer, (2012). Bonnet Carre Spillway. www.mvn.usace.army.mil/recreation

Wang, H., Steyer, G.D., Couvillion, B.R., Rybczyk J.M., Beck, H.J., Sleavin, W.J., Meselhe E.A., Allison, M.A., Boustany, R.G., Fischenich, C.J., and Rivera-Monroy, V.H. (2014). Forecasting landscape effects of Mississippi River diversions on elevation and accretion in Louisiana deltaic wetlands under future environmental uncertainty scenarios. Estuarine Coastal Shelf Science 138: 57-68.

Waters, J.P., Easley, D.H., Noakes, S.E., and Penland, S., (2009). Geochemistry of surficial sediments from Lake Pontchartrain resulting from the 1997 opening of the Bonnet Carré Spillway. Journal of Coastal Research 54: 127-140.

White, J.R., Reddy, K.R., and Moustafa, M.Z. (2004). Influence of hydrologic regime and vegetation on phosphorus retention in Everglades storm water treatment area wetlands. Hydrological Processes 18: 343-355.

APPENDIX A: MOISTURE CONTENT RELATIOSHIP VS. DISTANCE FROM THE BCS

A.1 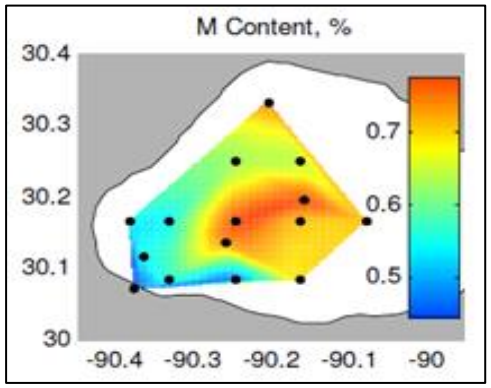

A.2 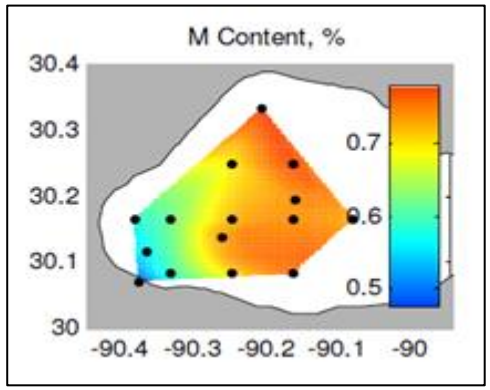

A.3 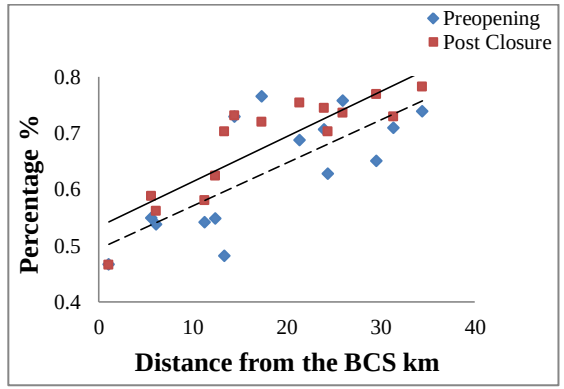

*Moisture content percentage map of Lake Pontchartrain from the 0-5 cm sediment interval before (A.1) and after (A.2) the 2011 BCS operation. Graph (A.3) of moisture content percentage vs. the distances from the BCS entrance to the LPE.

A.4 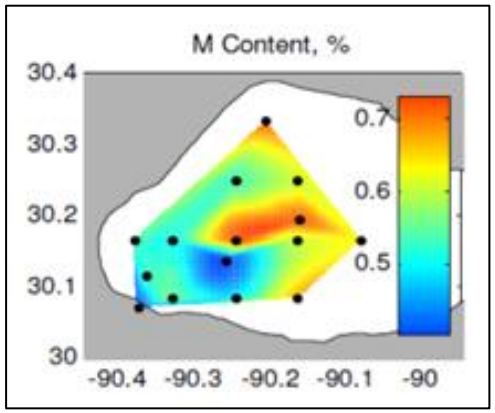

A.5 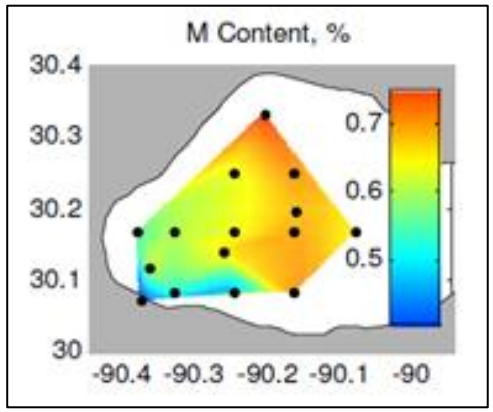

A.6 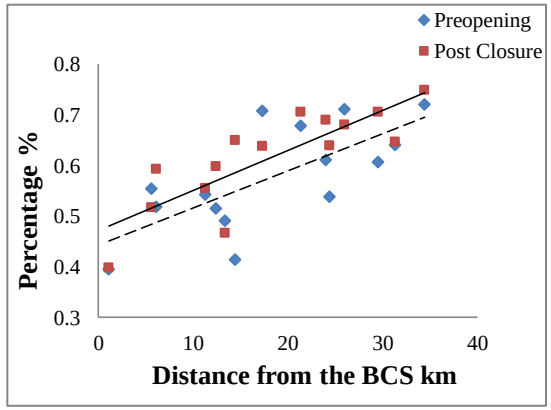

*Moisture content percentage map of Lake Pontchartrain from the 5-10 cm sediment interval before (A.4) and after (A.5) the 2011 BCS operation. Graph (A.6) of moisture content percentage vs. the distances from the BCS entrance to the LPE.

APPENDIX B: BULK DENSITY RELATIOSHIP VS. DISTANCE FROM THE BCS

B.1

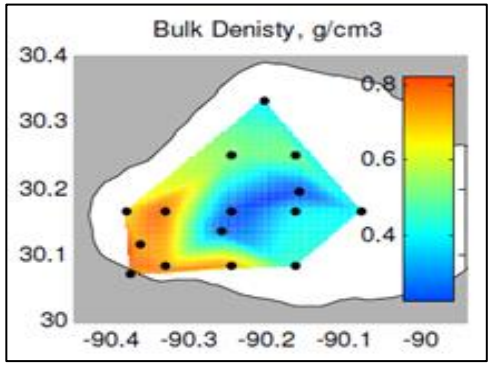

B.2

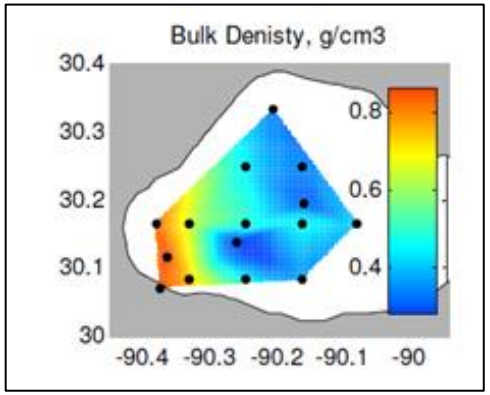

B.3

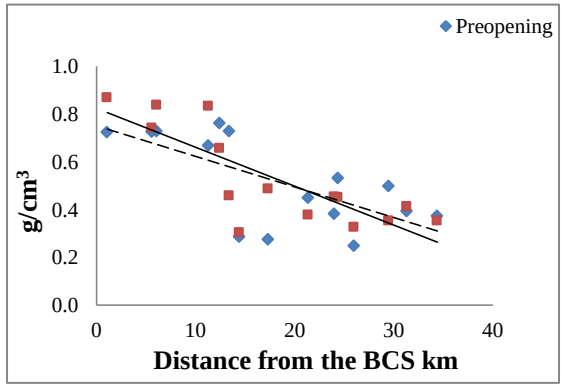

*Bulk density map of Lake Pontchartrain from the 0-5 cm sediment interval before (B.1) and after (B.2) the 2011 BCS operation. Graph (B.3) of bulk density vs. the distances from the BCS entrance to the LPE.

B.4

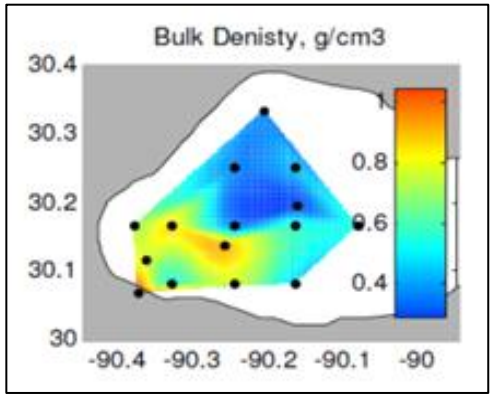

B.5

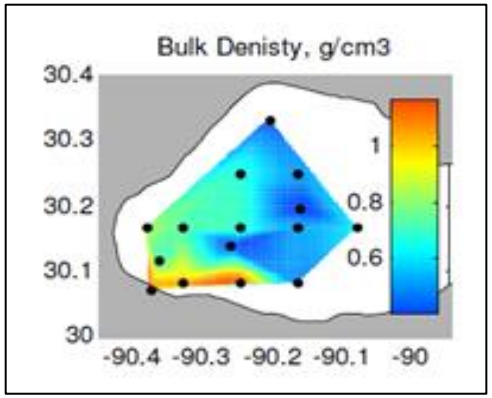

B.6

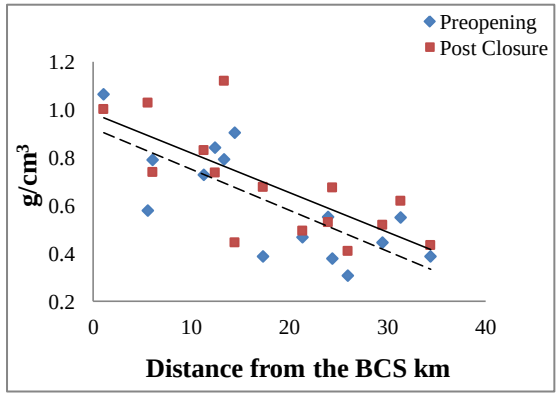

*Bulk density map of Lake Pontchartrain from the 5-10 cm sediment interval before (B.4) and after (B.5) the 2011 BCS operation. Graph (B.6) of bulk density vs. the distances from the BCS entrance to the LPE.

APPENDIX C: LOSS ON IGNITION RELATIOSHIP VS. DISTANCE FROM THE BCS

C.1 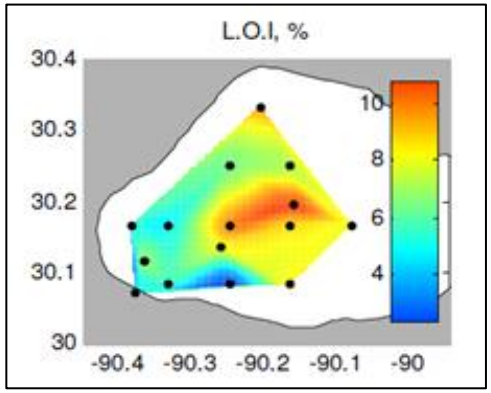

C.2 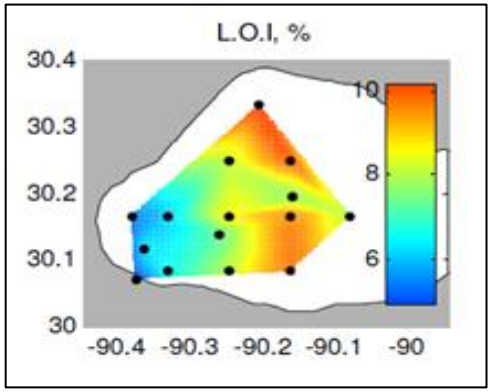

C.3 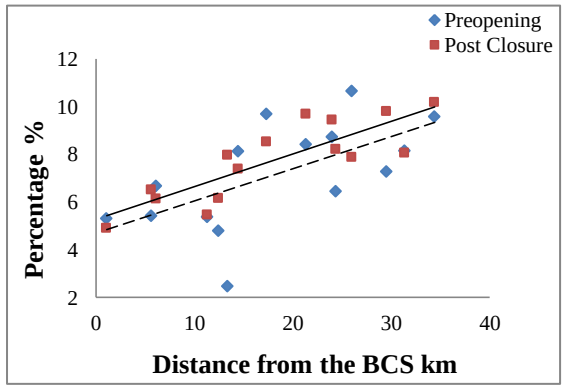

*Loss on ignition map of Lake Pontchartrain from the 0-5 cm sediment interval before (C.1) and after (C.2) the 2011 BCS operation. Graph (C.3) of loss on ignition vs. the distances from the BCS entrance to the LPE.

C.4 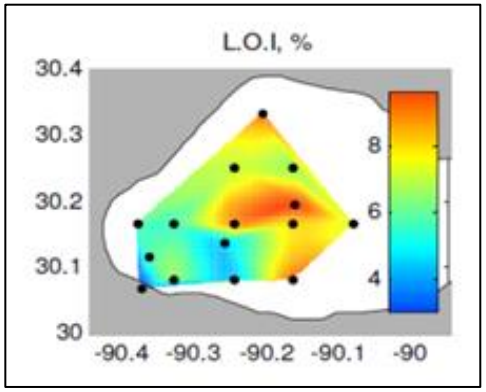

C.5 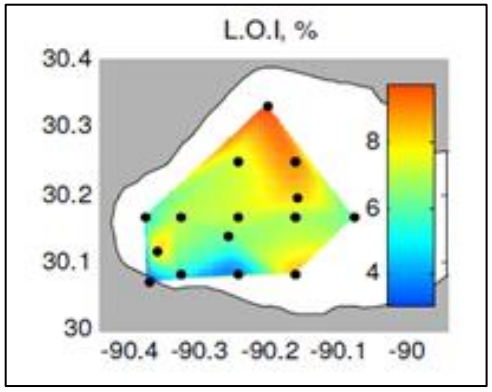

C.6 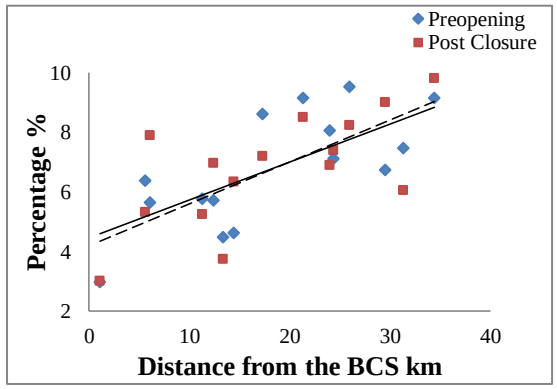

*Loss on ignition map of Lake Pontchartrain from the 5-10 cm sediment interval before (C.4) and after (C.5) the 2011 BCS operation. Graph (C.6) of loss on ignition vs. the distances from the BCS entrance to the LPE.

APPENDIX D: TOTAL CARBON CONCENTRATION RELATIONSHIP VS. DISTANCE FROM THE BCS

D.1 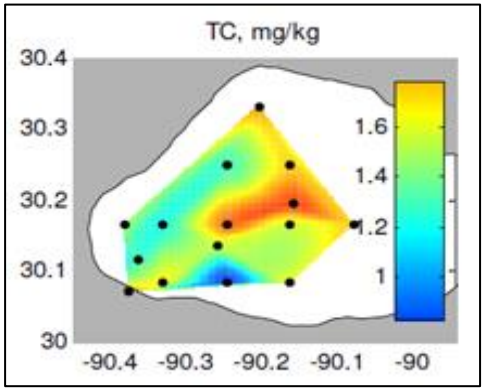

D.2 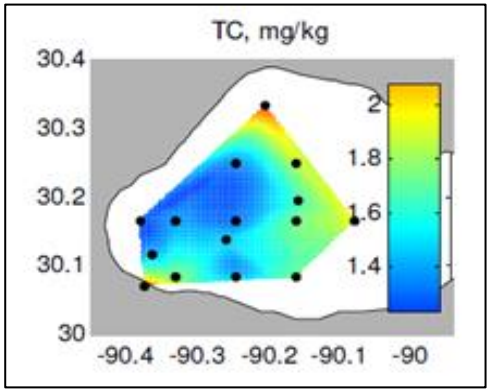

D.3 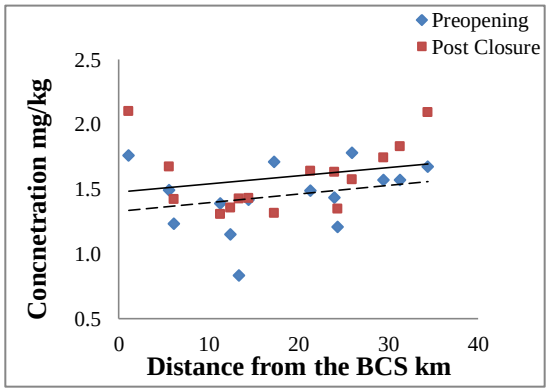

*Total carbon map of Lake Pontchartrain from the 0-5 cm sediment interval before (D.1) and after (D.2) the 2011 BCS operation. Graph (D.3) of total carbon concentration vs. the distances from the BCS entrance to the LPE.

D.4 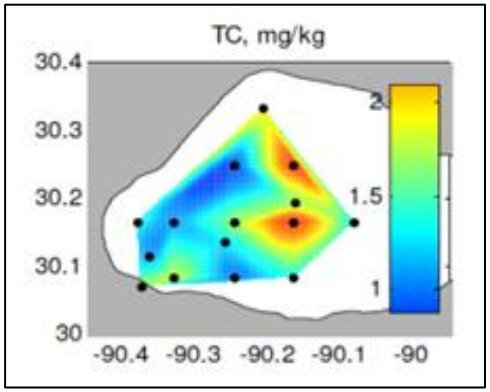

D.5 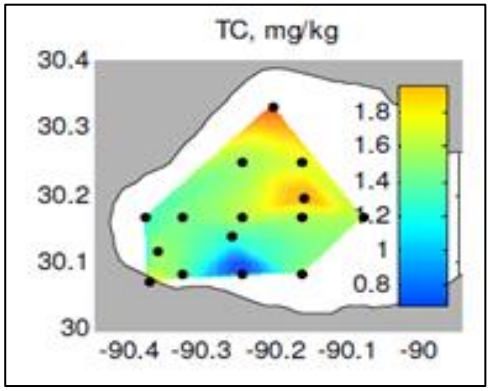

D.6 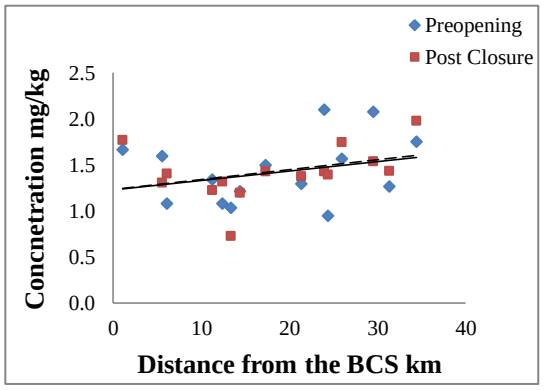

*Total carbon map of Lake Pontchartrain from the 5-10 cm sediment interval before (D.4) and after (D.5) the 2011 BCS operation. Graph (D.6) of total carbon concentration vs. the distances from the BCS entrance to the LPE.

APPENDIX E: TOTAL NITROGEN CONCENTRATION RELATIONSHIP VS. DISTANCE FROM THE BCS

E.1

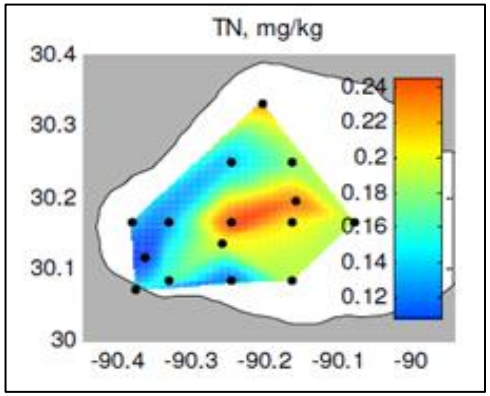

E.2

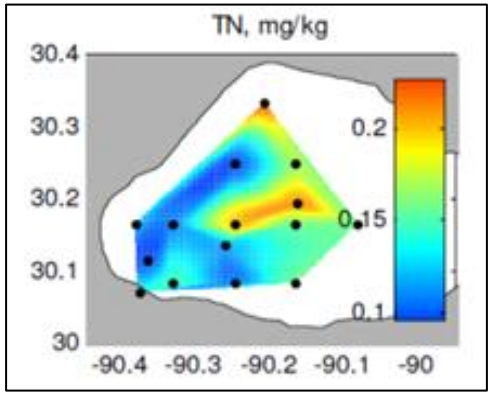

E.3

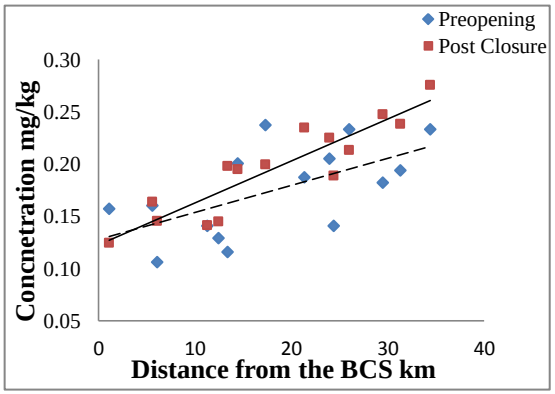

*Total nitrogen concentration map of Lake Pontchartrain from the 0-5 cm sediment interval before (E.1) and after (E.2) the 2011 BCS operation. Graph (E.3) of total nitrogen concentration vs. the distances from the BCS entrance to the LPE.

E.4

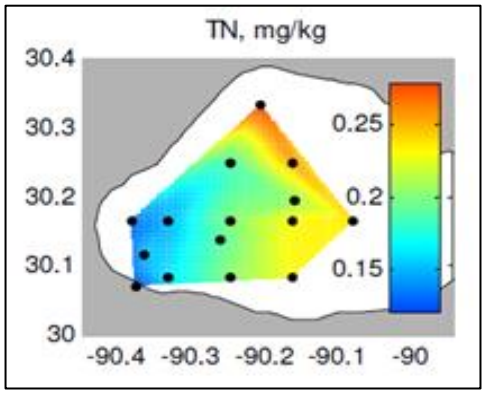

E.5

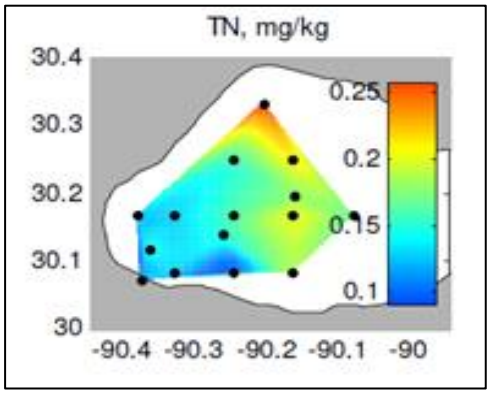

E.6

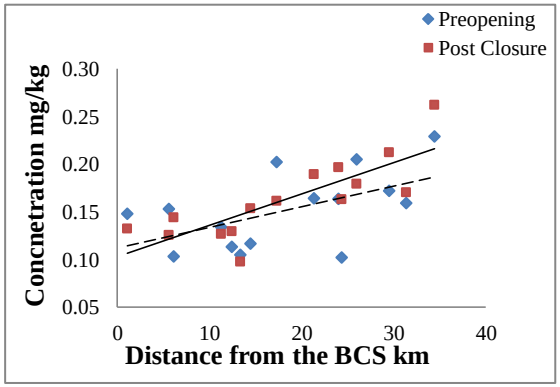

*Total nitrogen concentration map of Lake Pontchartrain from the 5-10 cm sediment interval before (E.4) and after (E.5) the 2011 BCS operation. Graph (E.6) of total nitrogen concentration vs. the distances from the BCS entrance to the LPE.

APPENDIX F: TOTAL PHOSPHORUS CONCENTRATION RELATIONSHIP VS. DISTANCE FROM THE BCS

F.1

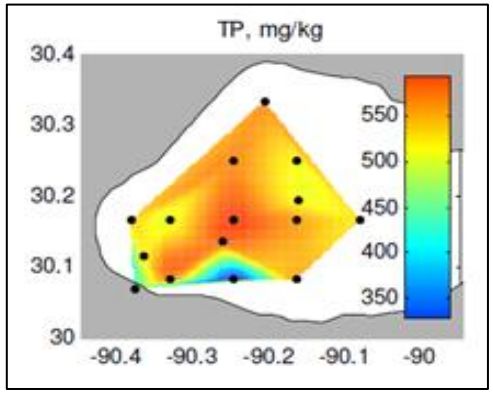

F.2

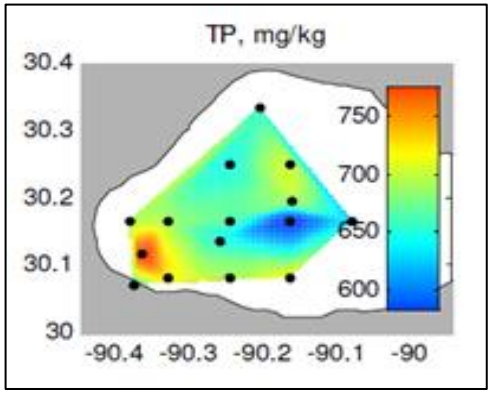

F.3

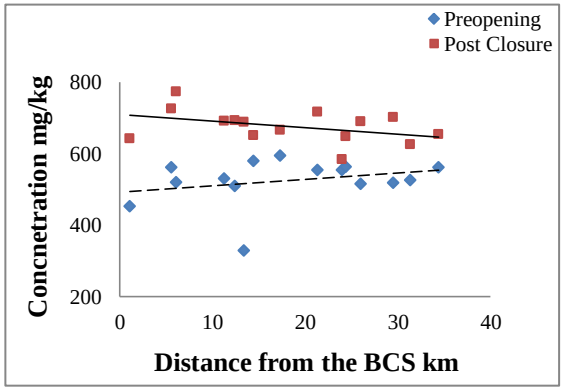

*Total phosphorus concentration map of Lake Pontchartrain from the 0-5 cm sediment interval before (F.1) and after (F.2) the 2011 BCS operation. Graph (F.3) of total phosphorus concentration vs. the distances from the BCS entrance to the LPE.

F.4

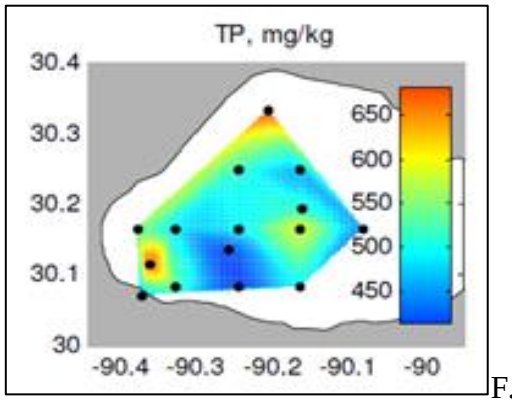

F.5

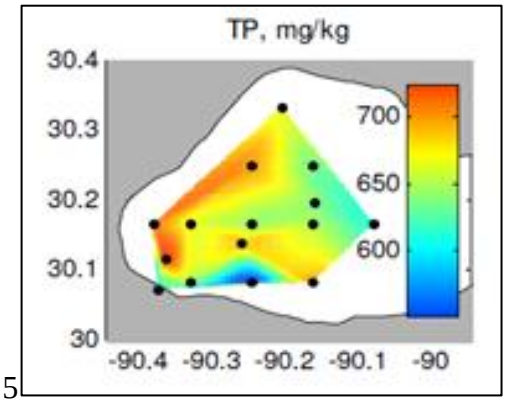

F.6

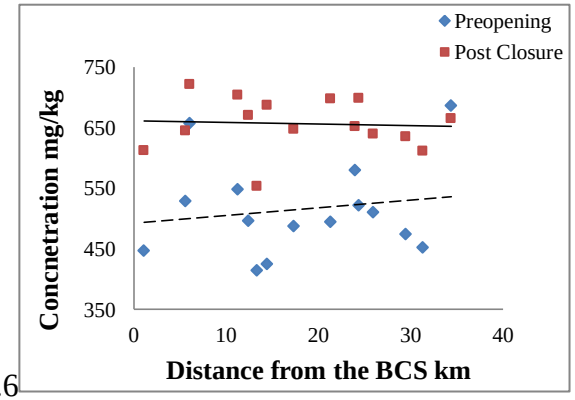

*Total phosphorus concentration map of Lake Pontchartrain from the 5-10 cm sediment interval before (F.4) and after (F.5) the 2011 BCS operation. Graph (F.6) of total phosphorus concentration vs. the distances from the BCS entrance to the LPE.

APPENDIX G: READILY AVAILABLE P CONCENTRATION RELATIONSHIP VS. DISTANCE FROM THE BCS

G.1 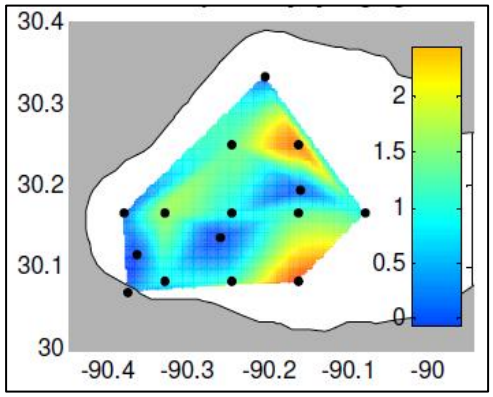

G.2 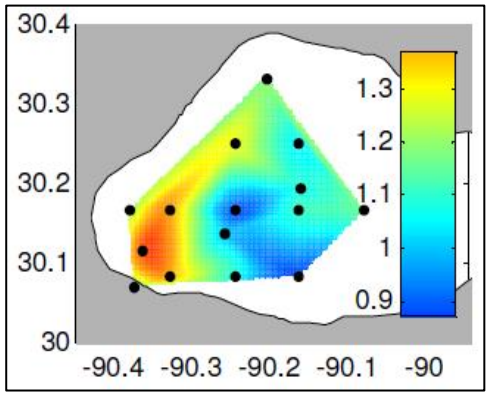

G.3 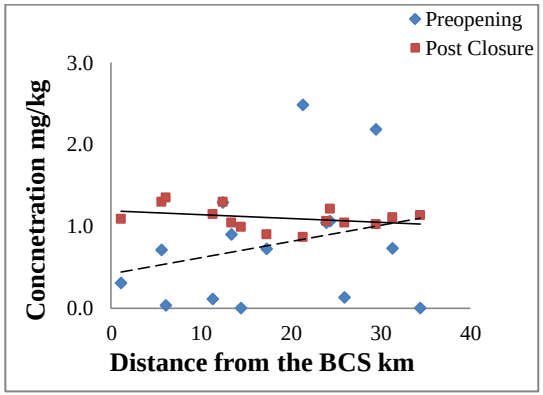

*Readily available P concentration map of Lake Pontchartrain from the 0-5 cm sediment interval before (G.1) and after (G.2) the 2011 BCS operation. Graph (G.3) of readily available P concentration vs. the distances from the BCS entrance to the LPE.

G.4 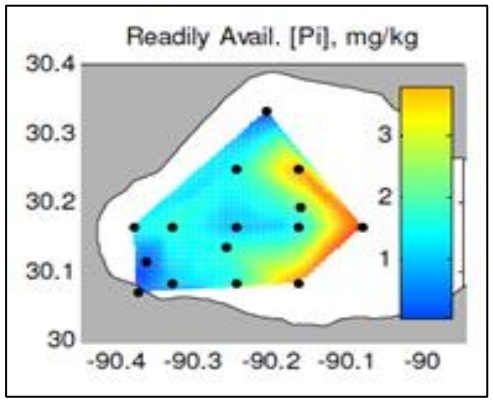

G.5 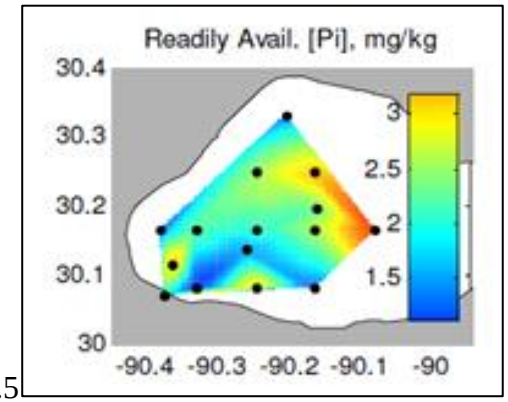

G.6 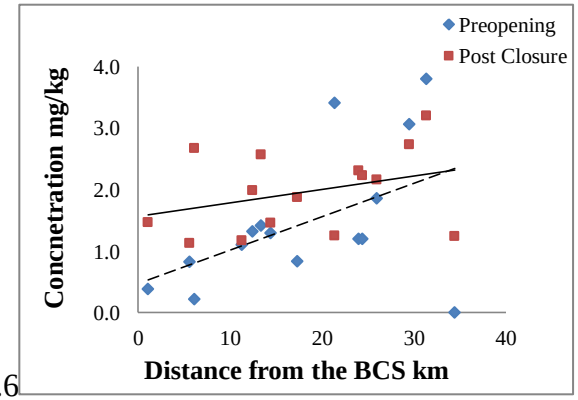

*Readily available P concentration map of Lake Pontchartrain from the 5-10 cm sediment interval before (G.4) and after (G.5) the 2011 BCS operation. Graph (G.6) of readily available P concentration vs. the distances from the BCS entrance to the LPE.

APPENDIX H: ALKALI ORGANIC P CONCENTRATION RELATIONSHIP VS. DISTANCE FROM THE BCS

H.1

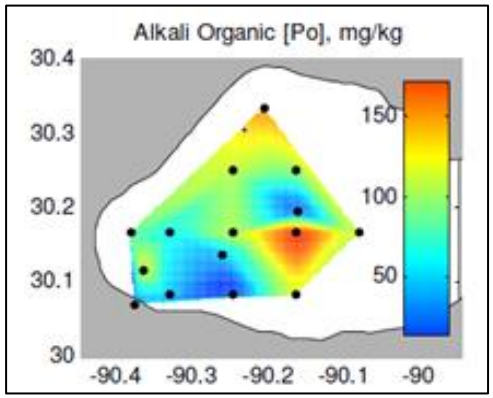

H.2

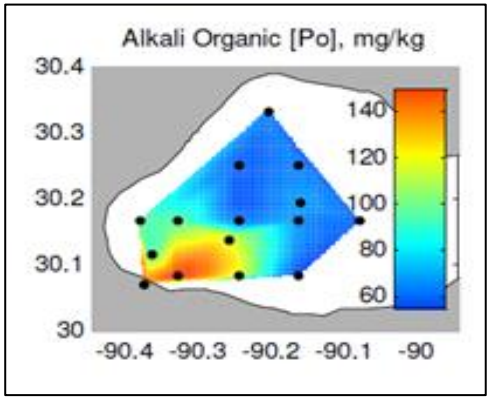

H.3

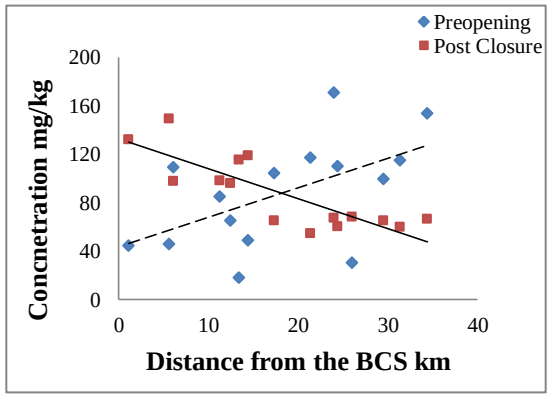

*Alkali organic P concentration map of Lake Pontchartrain from the 0-5 cm sediment interval before (H.1) and after (H.2) the 2011 BCS operation. Graph (H.3) of alkali organic P concentration vs. the distances from the BCS entrance to the LPE.

H.4

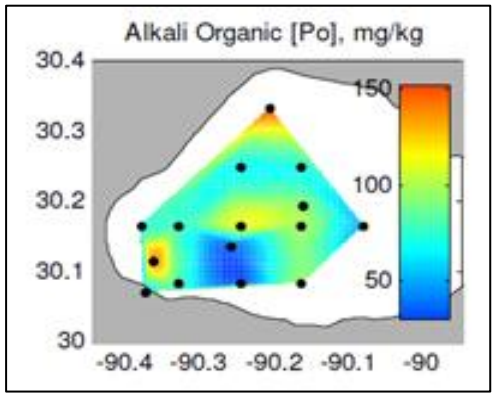

H.5

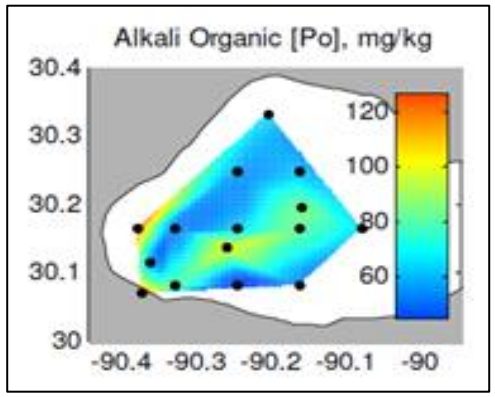

H.6

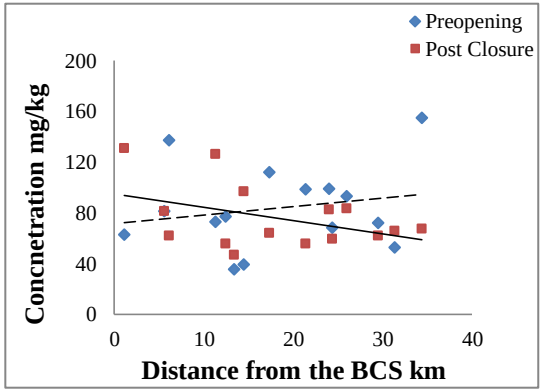

*Alkali organic P concentration map of Lake Pontchartrain from the 5-10 cm sediment interval before (H.4) and after (H.5) the 2011 BCS operation. Graph (H.6) of alkali organic P concentration vs. the distances from the BCS entrance to the LPE.

APPENDIX I: FE/AL BOUND P CONCENTRATION RELATIONSHIP VS. DISTANCE FROM THE BCS

I.1

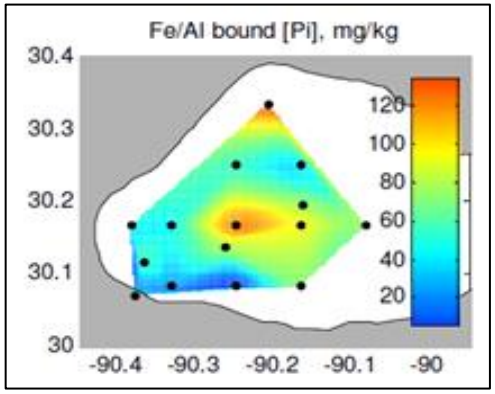

I.2

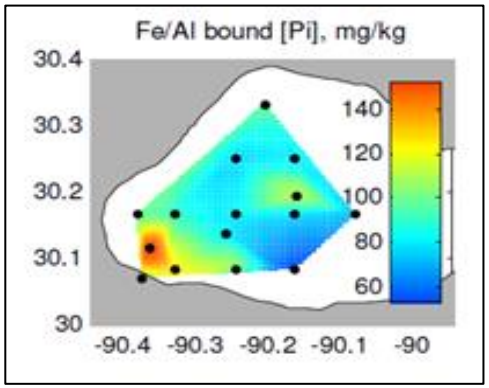

I.3

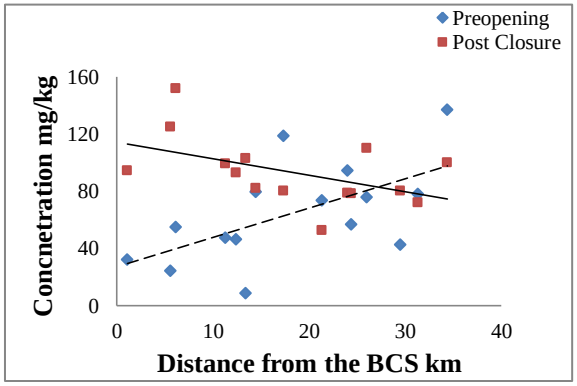

*Fe/Al bound P concentration map of Lake Pontchartrain from the 0-5 cm sediment interval before (I.1) and after (I.2) the 2011 BCS operation. Graph (I.3) of Fe/Al bound P concentration vs. the distances from the BCS entrance to the LPE.

I.4

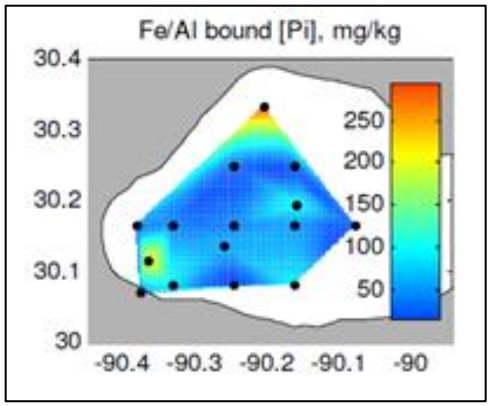

I.5

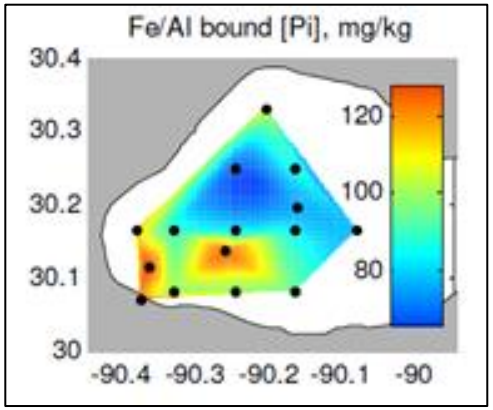

I.6

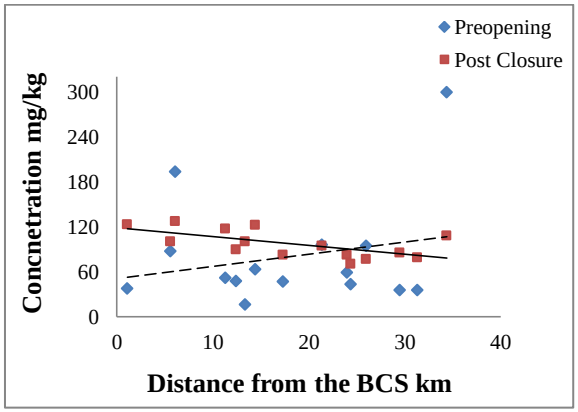

*Fe/Al bound P concentration map of Lake Pontchartrain from the 5-10 cm sediment interval before (I.4) and after (I.5) the 2011 BCS operation. Graph (I.6) of Fe/Al bound P concentration vs. the distances from the BCS entrance to the LPE.

APPENDIX J: CA/MG BOUND P CONCENTRATION RELATIONSHIP VS. DISTANCE FROM THE BCS

J.1

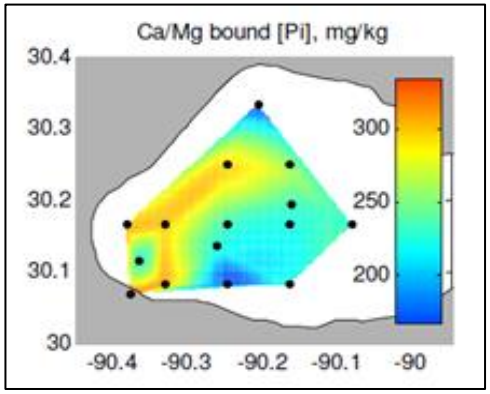

J.2

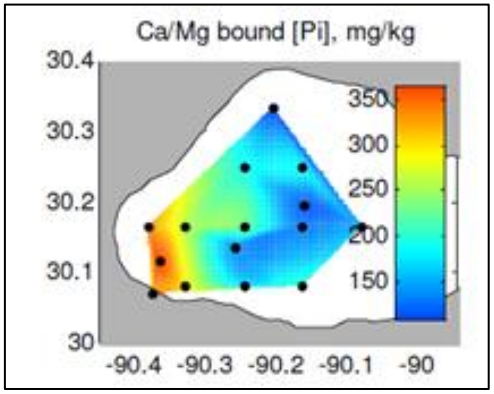

J.3

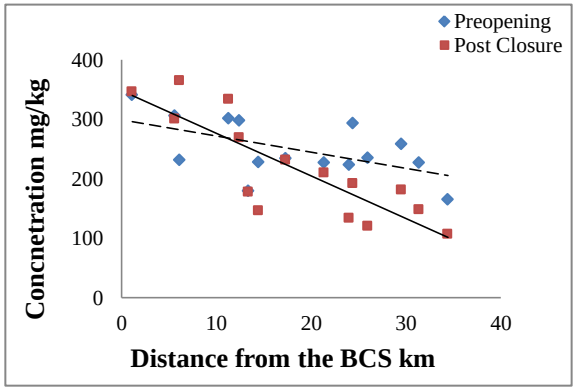

*Ca/Mg bound P concentration map of Lake Pontchartrain from the 0-5 cm sediment interval before (J.1) and after (J.2) the 2011 BCS operation. Graph (J.3) of Ca/Mg bound P concentration vs. the distances from the BCS entrance to the LPE.

J.4

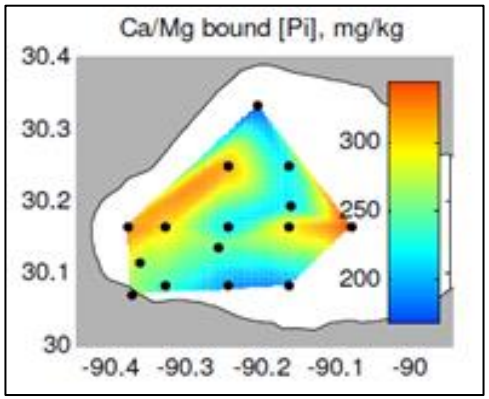

J.5

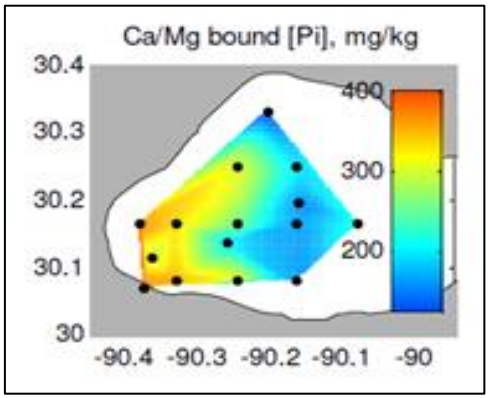

J.6

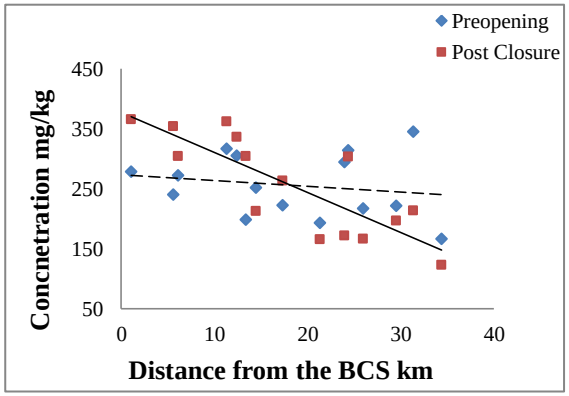

*Ca/Mg bound P concentration map of Lake Pontchartrain from the 5-10 cm sediment interval before (J.4) and after (J.5) the 2011 BCS operation. Graph (J.6) of Ca/Mg bound P concentration vs. the distances from the BCS entrance to the LPE.

APPENDIX K: RESIDUAL P CONCENTRATION RELATIONSHIP VS. DISTANCE FROM THE BCS

K.1 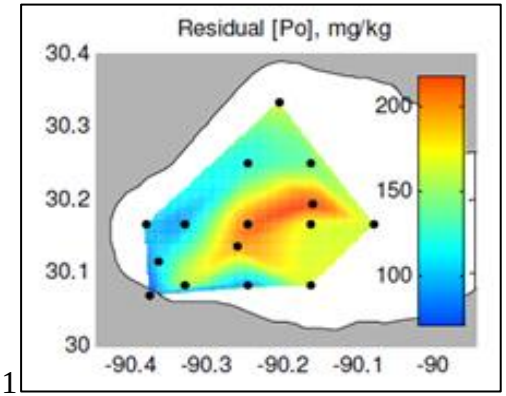

K.2 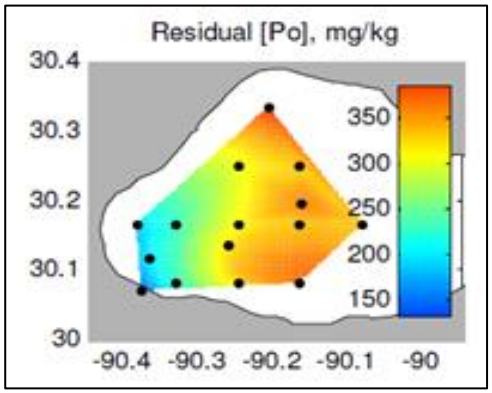

K.3 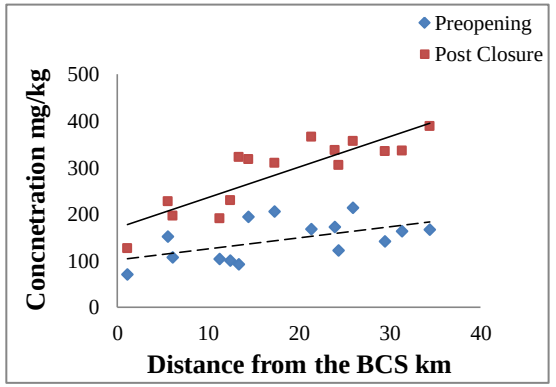

*Residual P concentration map of Lake Pontchartrain from the 0-5 cm sediment interval before (K.1) and after (K.2) the 2011 BCS operation. Graph (K.3) of residual P concentration vs. the distances from the BCS entrance to the LPE.

K.4 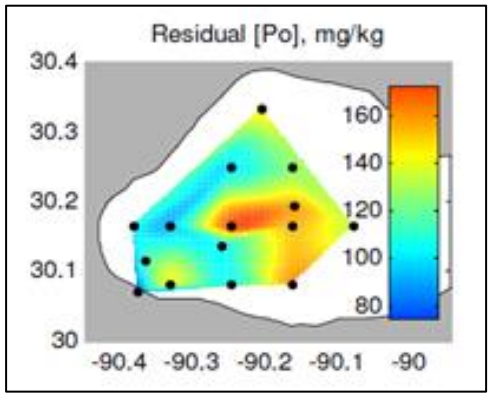

K.5 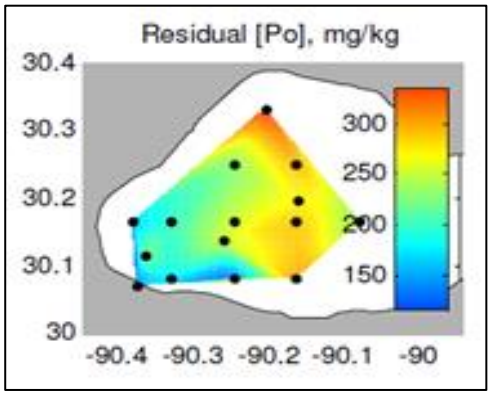

K.6 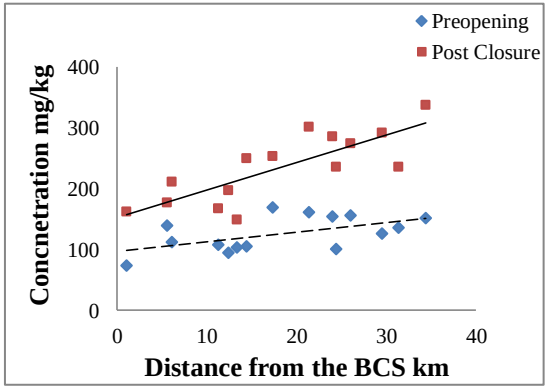

*Residual P concentration map of Lake Pontchartrain from the 5-10 cm sediment interval before (K.4) and after (K.5) the 2011 BCS operation. Graph (K.6) of residual P concentration vs. the distances from the BCS entrance to the LPE.

VITA

Nhan Thanh Nguyen was born in Can Tho, Vietnam, in 1989 and grew up in the Ascension Parish, Louisiana, USA. Growing up, he enjoyed exploring the outdoors, fishing, and playing sports. Nathan attended Louisiana State University and was involved with the Howard Hughes Medical Institute undergraduate research, Ronald McNair research scholars, and the Louisiana Sea Grant UROP research program, gaining laboratory and field experiences. He earned a Bachelor of Science degree in Chemistry with an Environmental concentration in 2012. Following graduation, Nathan began his Masters of Science degree in the Department of Oceanography and Coastal Sciences focusing on Wetland and Aquatic Biogeochemistry under Dr. John R. White at Louisiana State University.